Design

Modelling and

Experiments of

Advanced

Structures and

Systems

DeMEASS VIII

21 – 24 May, 2017
Izmailovo, Moscow

lims.tstu.ru/DEMEASS2017

Russian Science Foundation

International Conference

DeMEASS VIII

21-24 May 2017

Tambov Technical University

Chairman

Gennady M. Kulikov
Head of Laboratory of Intelligent Materials and Structures
Tambov State Technical University
Sovetskaya 106, Tambov 392000, Russia

Organizing Committee

Erasmo Carrera	DeMEASS I (2006)	Bardonecchia, Italy
Thomas Wallmersperger	DeMEASS II (2007)	Bad Herrenalb, Germany
Olivier Polit	DeMEASS III (2009)	Vernon, France
Salim Belouettar	DeMEASS IV (2011)	Urspelt, Luxemburg
Michael Krommer	DeMEASS V (2012)	Ulrichsberg, Austria
Roeland De Breuker	DeMEASS VI (2014)	Ede, The Netherlands
Thomas Wallmersperger	DeMEASS VII (2015)	Radebeul, Germany
Gennady Kulikov	DeMEASS VIII (2017)	Izmailovo, Russia

Local Organizing Committee

G. M. Kulikov (Chairman)
M. V. Shitikova
S. V. Plotnikova
N. A. Gunina
Phone: +7 910 750 2495

Conference Participants

Prof. Holm Altenbach
Otto-von-Guericke-Universität Magdeburg, Magdeburg, Germany

Dr. Aurelio Araujo
Universidade de Lisboa, Lisbon, Portugal

Naira Aslanyan
Shirak State University, Gyumri, Armenia

Dr. Salim Belouettar
Luxembourg Institute of Science and Technology, Luxembourg

Prof. Erasmo Carrera
Politecnico di Torino, Turin, Italy

Dr. Michele D'Ottavio
Université Paris Nanterre, Paris, France

Dr. Sascha Duczek
Otto-von-Guericke-Universität Magdeburg, Magdeburg, Germany

Fabian Duvigneau
Otto-von-Guericke-Universität Magdeburg, Magdeburg, Germany

Adrian Ehrenhofer
Technische Universität Dresden, Dresden, Germany

Hassan Elahi
Sapienza Università di Roma, Rome, Italy

Prof. Ulrich Gabbert
Otto-von-Guericke-Universität Magdeburg, Magdeburg, Germany

Prof. Dimitri Georgievskii
Lomonosov Moscow State University, Moscow, Russia

Dr. Gaetano Giunta
Luxembourg Institute of Science and Technology, Luxembourg

Dr. Nataliya Gunina
Tambov State Technical University, Tambov, Russia

Mario Kleo
Technische Universität Dresden, Dresden, Germany

Prof. Gennady Kulikov
Tambov State Technical University, Tambov, Russia

Thi Huyen Cham Le
Université Paris Nanterre, Paris, France

Peter Leichsenring
Technische Universität Dresden, Dresden, Germany

Prof. Jose Madeira
Universidade de Lisboa, Lisbon, Portugal

Jonas Maruani
Université Paris Nanterre, Paris, France

Prof. Gennadi Mikhasev
Belarusian State University, Minsk, Belarus

Prof. Andrey Nasedkin
Southern Federal University, Rostov-on-Don, Russia

Dr. Svetlana Plotnikova
Tambov State Technical University, Tambov, Russia

Prof. Olivier Polit
Université Paris Nanterre, Paris, France

Dr. Eric Puntel
Università di Udine, Udine, Italy

Dr. António Ribeiro
Universidade de Lisboa, Lisbon, Portugal

Marco Rossi
Technische Universität Dresden, Dresden, Germany

Content

Bending of a Three-Layered Plate with Surface Stresses

Holm Altenbach and Victor A. Eremeyev

Abstract We discuss here the bending deformations of a three-layered plate taking into account surface and interfacial stresses. The first-order shear deformation plate theory and the Gurtin-Murdoch model of surface stresses will be considered and the formulae for stiffness parameters of the plate are derived. Their dependence on surface elastic moduli will be analyzed.

Recently with respect to developments in the technologies of nanostructured materials the interest grows to surface elasticity and models which explicitly take into account surface stresses. For example, the model Gurtin and Murdoch presented in [5, 6] found many applications in micro- and nanomechanics, see [3, 9, 4] and the reference therein. In particular, it can forecast the positive size-effect. The Gurtin-Murdoch model is also used for modification of models of plates and shells to the nanoscale, see for example [1, 2, 8]. Here we discuss the dependence of elastic properties including bending stiffness of an elastic three-layered plate with interfacial and surface stresses acting on layer interfaces and plate faces.

The equilibrium equations and the boundary conditions take the following form:

$$\nabla_{\mathbf{x}} \cdot \mathbf{P} + \rho \mathbf{f} = \mathbf{0}, \quad \mathbf{x} \in V, \quad (\mathbf{n} \cdot \mathbf{P} - \nabla_{\mathrm{s}} \cdot \mathbf{S})|_{\Omega_s} = \mathbf{t}, \quad \mathbf{u}|_{\Omega_u} = \mathbf{u}_0, \quad \mathbf{n} \cdot \mathbf{P}|_{\Omega_f} = \mathbf{t}. \tag{1}$$

Here $\mathbf{P}$ is the stress tensor, $\nabla_{\mathbf{x}}$ the three-dimensional (3D) nabla operator, ∇_{s} the surface (2D) nabla operator, $\mathbf{S}$ the surface stress tensor acting on the surfaces Ω_{s}, $\mathbf{u}$ the displacement vector, $\mathbf{f}$ and $\mathbf{t}$ the body force and surface force vectors, respectively, and ρ the mass density. On Ω_u the displacements are given, whereas on Ω_f the surface stresses $\mathbf{S}$ are absent, $\Omega \equiv \partial V = \Omega_u \cup \Omega_{\mathrm{s}} \cup \Omega_f$, V is the body volume,

Holm Altenbach
Otto-von-Guericke-Universität Magdeburg, Universitätsplatz 2, D-39106 Magdeburg, Germany,
e-mail: holm.altenbach@ovgu.de

Victor A. Eremeyev
Rzeszow University of Technology, al. Powstańców Warszawy 8, 35959 Rzeszów, Poland,
and South Federal University, Milchakova str. 8a, 344090 Rostov on Don, Russia,
e-mail: eremeyev.victor@gmail.com

and $\mathbf{x}$ is the position vector. Tensors $\mathbf{S}$ and $\mathbf{P}$ are given by

$$\mathbf{P} = \lambda \mathbf{I}\mathrm{tr}\mathbf{E} + 2\mu\mathbf{E}, \quad \mathbf{S} = \mathbf{S}_0 + 2\mu_s\mathbf{e} + \lambda_s\mathbf{A}\mathrm{tr}\mathbf{e} + \mathbf{S_0}\cdot\nabla_s\mathbf{u}, \tag{2}$$

where

$$\mathbf{E} = \frac{1}{2}\left[\nabla\mathbf{u} + (\nabla\mathbf{u})^{\mathrm{T}}\right], \quad \mathbf{e} = \frac{1}{2}\left[\nabla_s\mathbf{u}\cdot\mathbf{A} + \mathbf{A}\cdot(\nabla_s\mathbf{u})^{\mathrm{T}}\right],$$

$\mathbf{A} \equiv \mathbf{I} - \mathbf{n}\otimes\mathbf{n}$, $\mathbf{I}$ the 3D unit tensor, $\mathbf{S}_0$ the initial surface stress tensor, λ, μ, λ_s and μ_s are the classic and surface Lamé moduli, respectively.

Applying the through-the-thickness integration technique of [7] to plate-like bodies with surface stresses, we obtain the 2D constitutive equations for nano-sized plates and shells as follows [1, 2]: $\mathbf{T}^* = \mathbf{T} + \mathbf{T}_s$, $\mathbf{M}^* = \mathbf{M} + \mathbf{M}_s$, where $\mathbf{T}$ and $\mathbf{M}$ are the stress and couple stress resultant tensors, respectively. $\mathbf{T}$ and $\mathbf{M}$ are the classical resultant tensors, while $\mathbf{T}_s$ and $\mathbf{M}_s$ are resultant tensors induced by surface stresses $\mathbf{S}$ acting on the faces and interfaces. For infinitesimal deformations tensors $\mathbf{T}^*$ and $\mathbf{M}^*$ are linear tensor-valued functions of the following strain measures

$$\mathbf{e} = \frac{1}{2}\left(\nabla_s\mathbf{v} + (\nabla_s\mathbf{v})^{\mathrm{T}}\right), \quad \mathbf{k} = \frac{1}{2}\left(\nabla_s\mathbf{g} + (\nabla_s\mathbf{g})^{\mathrm{T}}\right), \quad \mathbf{G} = \nabla_s w - \mathbf{g}, \tag{3}$$

where $\mathbf{w}$ and $\mathbf{g}$ are the displacements and rotations, $\mathbf{v} = \mathbf{w}\cdot\mathbf{A}$, $w = \mathbf{w}\cdot\mathbf{n}$, and for isotropic plates are the following relations valid

$$\mathbf{T}^*\cdot\mathbf{A} = C_1\mathbf{e} + C_2\mathbf{A}\mathrm{tr}\mathbf{e}, \quad \mathbf{M}^* = [D_1\mathbf{k} + D_2\mathbf{A}\mathrm{tr}\mathbf{k}]\times\mathbf{n}, \quad \mathbf{T}^*\cdot\mathbf{n} = \Gamma\mathbf{G}. \tag{4}$$

Here $\mathbf{n}$ is the unit normal vector to the plate. In what follows we discuss the dependence of stiffness parameters C_1, C_2, D_1, D_2, and Γ on the surface elastic moduli and layer thicknesses.

References

1. Altenbach, H., Eremeev, V.A., Morozov, N.F.: On equations of the linear theory of shells with surface stresses taken into account. Mech Solids **45**(3), 331–342 (2010)
2. Altenbach, H., Eremeyev, V.A.: On the shell theory on the nanoscale with surface stresses. Int J Engng Sci **49**(12), 1294–1301 (2011)
3. Duan, H., Wang, J., Karihaloo, B.L.: Theory of elasticity at the nanoscale. Adv Appl Mech **42**, 1–68 (2009)
4. Eremeyev, V.A.: On effective properties of materials at the nano-and microscales considering surface effects. Acta Mech **227**(1), 29–42 (2016)
5. Gurtin, M.E., Murdoch, A.I.: A continuum theory of elastic material surfaces. Arch Ration Mech Anal **57**(4), 291–323 (1975)
6. Gurtin, M.E., Murdoch, A.I.: Surface stress in solids. Int J Solids Struct **14**(6), 431–440 (1978)
7. Libai, A., Simmonds, J.G.: The Nonlinear Theory of Elastic Shells, 2nd edn. Cambridge University Press, Cambridge (1998)
8. Ru, C.Q.: A strain-consistent elastic plate model with surface elasticity. Continuum Mechanics and Thermodynamics **28**(1–2), 263–273 (2016)
9. Wang, J., Huang, Z., Duan, H., Yu, S., Feng, X., Wang, G., Zhang, W., Wang, T.: Surface stress effect in mechanics of nanostructured materials. Acta Mech Solida Sin **24**(1), 52–82 (2011)

Model of Thermoelasticity of Micropolar Plates and Beams with Constrained Rotation

N. Aslanyan[1], S. Sargsyan[1]

[1] Shirak State University after M. Nalbandyan, P. Sevak 4, 3126, Gyumri, Armenia

Abstract

Developing the approach of paper [1] mathematical models of thermoelasticity of micropolar thin beams and plates with constrained rotation are constructed on the basis of which solutions of some applied problems are studied. With the help of numerical analysis of these problems effective properties of rigidity of micropolar material of the beam or plate are stated compared with the classical material.

1 Model of Thermoelasticity of Micropolar Thin Beams with Constrained Rotation

The constructed model of thermoelasticity of micropolar thin bemas with constrained rotation is expressed as follows:

Equilibrium equtions

$$\frac{dN_{12}}{dx_1}=-q_{x_2},\qquad N_{21}-\frac{dM_{11}}{dx_1}=hq_{x_1},\qquad \frac{dL_{13}}{dx_1}+N_{12}-N_{21}=-m. \tag{1}$$

Physical relations of thermoelasticity

$$N_{12}+N_{21}=4\mu h\tilde{\Gamma}_{12},\ \ M_{11}=\frac{2Eh^3}{3}\left(K_{11}-\alpha_t\chi_t\right),\ \ L_{13}=2hBk_{13},\ \ \chi_t=\frac{\tilde{T}}{2h}. \tag{2}$$

Geometrical relations

$$K_{11}=\frac{d\psi}{dx_1},\ \tilde{\Gamma}_{12}=\frac{dw}{dx_1}+\psi,\ k_{13}=\frac{d\Omega_3}{dx_1},\ \Omega_3(x_1)=\frac{1}{2}\left(\frac{dw}{dx_1}-\psi\right). \tag{3}$$

Here N_{12}, N_{21} are forces, M_{11}, L_{13} are moments of force and moment stresses, $\tilde{\Gamma}_{12}$ is the shear deformation, K_{11} и k_{13} are the bending axes of the beam from corresponding stresses, w is the deflection of the beam, ψ is the angle of rotation of the normal cross section, Ω_3 is the angle of its free rotation, E,μ,B are the elastic constants, $T=x_2\frac{\tilde{T}}{2h}$, T is the temperature, $2h$ is the thickness of the beam, α_t is the coefficient of linear expansion. On each side of the beam ($x_1=0, x_2=a$) three boundary conditions should take place.

Numerical results are introduced: when two edges of the beam are hinged supported; $\delta=\frac{h}{a}=\frac{1}{40}, T_0=60^\circ C$, $\alpha_t=125\times10^{-7}\ {}^1\!/_{\deg}$, $\frac{\overline{w}_{\max}^{mik}}{\overline{w}_{\max}^{kl}}=0.97$ when $B^*=1.5\times10^{-5}$, $\frac{\overline{w}_{\max}^{mik}}{\overline{w}_{\max}^{kl}}=0.79$ when $B^*=1.5\times10^{-4}$, $\frac{\overline{w}_{\max}^{mik}}{\overline{w}_{\max}^{kl}}=0.27$ when $B^*=1.5\times10^{-3}$. As we can see from the results, in case of increase of dimensionless micropolar constant B^* rigidity of the beam is increased.

2 Model of Thermoelasticity of Micropolar Thin Plates with Constrained Rotation

The constructed model of thermoelasticity of micropolar thin bemas with constrained rotation is expressed as follows:

Equilibrium equtions

$$\frac{\partial N_{13}}{\partial x_1}+\frac{\partial N_{23}}{\partial x_2}=-\tilde{p}_3, \qquad N_{3i}-\left(\frac{\partial M_{ii}}{\partial x_i}+\frac{\partial M_{ji}}{\partial x_j}\right)=h\tilde{p}_i$$
$$\frac{\partial L_{ii}}{\partial x_i}+\frac{\partial L_{ji}}{\partial x_j}+(-1)^j\left(N_{j3}-N_{3j}\right)=-\tilde{m}_i, \qquad \frac{\partial \Lambda_{13}}{\partial x_1}+\frac{\partial \Lambda_{23}}{\partial x_2}+(M_{12}-M_{21})=0. \tag{4}$$

Physical relations of thermoelasticity

$$N_{i3}+N_{3j}=4\mu h\left(\Gamma_{i3}+\Gamma_{3j}\right), \quad L_{ij}=2h\left[(\gamma+\varepsilon)k_{ij}+(\gamma-\varepsilon)k_{ji}\right], \quad L_{ii}=4\gamma hk_{ii}, \tag{5}$$
$$M_{11}=\frac{2Eh^3}{3(1-\nu^2)}\left[K_{ii}+\nu K_{jj}-(1+\nu)\alpha_t\chi_t\right],\ M_{12}+M_{12}=\frac{2\mu h^3}{3}\left[K_{12}+K_{21}\right],\ \Lambda_{i3}=\frac{2h^3}{3}\frac{4\gamma\varepsilon}{\gamma+\varepsilon}l_{i3}.$$

Geometrical relations

$$\Gamma_{i3}+\Gamma_{3j}=\frac{\partial w}{\partial x_1}+\psi_i,\ K_{ii}=\frac{\partial \psi_i}{\partial x_i},\quad K_{12}+K_{21}=\frac{\partial \psi_1}{\partial x_2}+\frac{\partial \psi_2}{\partial x_1},\ k_{ii}=\frac{\partial \Omega_i}{\partial x_i},\ \ k_{ij}=\frac{\partial \Omega_j}{\partial x_i},$$
$$\Omega_i=-\frac{1}{2}(-1)^j\left(\psi_j-\frac{\partial w}{\partial x_j}\right), \iota=\frac{1}{2}\left(\frac{\partial \psi_2}{\partial x_1}-\frac{\partial \psi_1}{\partial x_2}\right), l_{i3}=\frac{\partial \iota}{\partial x_i}. \tag{6}$$

On each side of the plate five boundary conditions should take place.
Numerical results are introduced: when edges of the plate are hinged supported; $\frac{\overline{w}_{\max}^{mik}}{\overline{w}_{\max}^{kl}}=0.49$ when $\overline{\gamma}=\overline{\varepsilon}=10^{-5}$, $\frac{\overline{w}_{\max}^{mik}}{\overline{w}_{\max}^{kl}}=0.31$ when $\overline{\gamma}=\overline{\varepsilon}=10^{-3}$, $\frac{\overline{w}_{\max}^{mik}}{\overline{w}_{\max}^{kl}}=0.25$ when $\overline{\gamma}=\overline{\varepsilon}=10^{-1}$.

3 Conclusion

Applied mathematical models of thermoelasticity of micropolar thin beams and plates with constrained rotation are constructed. Concrete problems of thermoelastic bending of micropolar thin beams and plates are solved. Analysis of the numerical results states effective properties of micropolar material from the point of view of rigidity of these thin bodies compared with the classical model.

References

[1] S. Sargsyan, Mathematical Model of Micropolar Thermo-Elasticity of Thin Shells: Journal of Thermal Stresses, 2013, vol.36, № 11, P.1200-1216.

Multi-scale composite material selection and design with a seamless integration of materials models and multidisciplinary design optimisation Case of the H2020 COMPOSELECTOR project

S. Belouettar[1*], G. Giunta[1], A. Daouadji[2]

[1] Luxembourg Institute of Science and Technology, Luxembourg

[2] INSA-LYON, University of Lyon, France

Abstract

The integration of modelling and simulations techniques to support material selection and design process is more and more impelling in the materials science and industrial domains, due to the need of effectively designing and producing increasingly sophisticated materials, components and systems with advanced performance on a competitive time scale. In this perspective, for complex structural materials there is a particular need in industry for chemistry/physics-based materials models and modelling workflows that fulfil the following requirements: i) predicting relevant properties and key performance indicators that capture the performance of materials, accounting for material internal microstructure and effects of processing and ii) accuracy/validation of predicted data, and relevant management of uncertainty. Materials selection and structural design are fundamentally goal-oriented, aimed at identifying material structures and processing paths that deliver required properties and performance. To be reliable, this process must be built upon a physical and engineering framework and based upon methods that are systemic, effective and efficient in modelling complex, hierarchical materials. For material design and selection, understanding and quantifying the links between material microstructure and their macroscopic effects is, therefore, essential. In parallel, high performance requires not only comprehensive material properties modelling but also understanding of risks, costs, and business opportunities for a range of decisions, from material selection to designing functional structural components and systems, and for process optimization. Last but not least, design and selection of must also accommodate societal requirements for health and sustainability. In my presentation, I will talk about the connection between material modelling and business processes where the coupling between performance, material, manufacturing process, cost, market and societal requirements constraints are exploited.
The main objective of COMPOSELECTOR is the development of a Business Decision Support System, which integrates materials modelling, business tools and databases into a single workflow to support the complex decision process involved in the selection and design of polymer-matrix composites. This will be achieved by means of an open platform which will enable interoperability and information management of materials models and data, connecting a rich material modelling layer with industry standard business process

[*] Corresponding author: S. Belouettar, e-mail: salim.belouettar@list.lu

models. Companies using the COMPOSELECTOR decision system will be able to control, manage and automate the repeatable decisions which are central to its business by effectively applying business rules, analytics, simulation and multi-objective optimization technologies cantered around the innovative concept of business “Apps”.

COMPOSELECTOR will produce high impact innovative technical solutions that will generate sustained competitive advantages in the domain of materials market in general and composite materials in particular. The computational framework will link various time and length scales ranging from nanoscale to macro-scale or from fundamental physics to the design of new polymer composites and structures. The combination of multi-level simulation, multi-objective optimization and its innovative association with business processes and decision-making abilities, will significantly improve the business and computational state-of-the-art tools available on the market.

NODE-DEPENDENT KINEMATIC SHELL ELEMENTS FOR THE ANALYSIS OF SMART STRUCTURES

E. Carrera[1], S. Valvano[1], G.M. Kulikov[2]

(1) Department of Mechanical and Aerospace Engineering, Politecnico di Torino
Corso Duca degli Abbruzzi 24, 10129, Turin, Italy
stefano.valvano, erasmo.carrera {@polito.it} www.mul2.com

(2) Department of Applied Mathematics and Mechanics, Tambov State Technical University
Sovetskaya Street 106, 392000 Tambov, Russia
kulikov@apmath.tstu.ru

Keywords: Node-Dependent Kinematics, Shell, Piezoelectric materials, Multifield problems, Unified Formulation.

Abstract

In the present work, a new class of shell finite elements is proposed for the static analysis of composite multilayered structures embedding piezoelectric layers as actuators and sensors. The accurate description of the mechanical and electric fields along the multilayer is ensured by the shell Finite Elements (FE) with equivalent-single-layer and layer-wise capabilities. The novelty of the present shell element consists in the use of node-dependent shell theory assumptions. The new finite element allows for the simultaneous analysis of different subregions of the problem domain with different kinematics and accuracy, in a global/local sense, see Fig. 1. The structural theory of the shell element is a property of the FE node in this present approach, and the continuity between two adjacent elements is ensured by adopting the same kinematics at the interface nodes. The main advantage of the present node-dependent variable kinematics element is that no ad-hoc techniques and mathematical artifices are required to mix the fields coming from two different and kinematically incompatible adjacent elements, because the shell structural theory varies within the finite element itself. It is possible to reduce the computational costs by assuming refined theories only in those zones/nodes of the structural domain where the resulting strain and stress states present a complex distribution. At the same time, computationally cheaper, low-order models can be used in the remaining parts of the shell where a localized detailed analysis is not necessary. The governing equations are derived using the Principle of Virtual Displacements (PVD) extended to the electro-mechanical case. This model has already shown good results in the mechanical analysis of multilayered composite plates[1], and in the mechanical analysis of complex structures by the use of one-dimensional node-dependent kinematics for the coupling of beam models[2]. The Mixed Interpolated Tensorial Components (MITC) method is employed to contrast the shear locking phenomenon that usually affects shell finite elements. One of the most interesting features of the unified formulation consists in the possibility to keep the order of the expansion of the state variables along the thickness of the shell as a parameter of the model.With node-dependent kinematics it is possible to keep the order of the expansion of the

state variables and models along the main reference plane of the shell structure as a parameter of the model. The electrical potential assumption for the layered actuators and sensors has been extended, from a layer-wise (LW) modeling, to an equivalent-single-layer (ESL) description, in the same way the displacements assumptions on the composite layers are described by a ESL and LW models. Some results from the static analysis of shells under electro-mechanical loads will be provided, in order to show the efficiency of models presented.

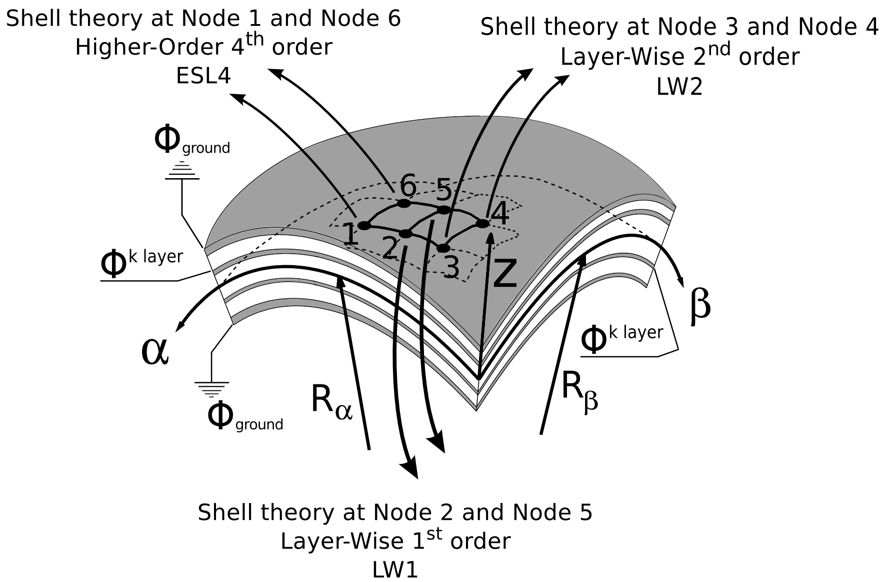

Figure 1: Node-dependent kinematic finite element example for a composite multilayered shell with piezoelectric layers.

References

[1] Carrera E., Pagani A., Valvano S., "Multilayered plate elements accounting for refined theories and node-dependent kinematics," *Composites Part B*, (Under Review).

[2] Carrera E., Zappino E., "Analysis of Complex Structures Coupling Variable Kinematics One-Dimensional Models," *ASME 2014 International Mechanical Engineering Congress and Exposition*, Montreal, Quebec, Canada, 14-20 November 2014.

An Abaqus Implementation of the Finite Cell Method to Analyse the Influence of Pores on the Strengths of Aluminum Die Cast Components

S. Duczek[1], M. Würkner[1], A. Abedian[2], H. Köppe[1], H. Berger[1], A. Düster[2] and U. Gabbert[1]

[1] Otto von Guericke University Magdeburg, Universitätsplatz 2, 39106 Magdeburg, {sascha.duczek;mathias.wuerkner;heinz.koeppe;harald.berger;ulrich.gabbert}@ovgu.de

[2] Hamburg University of Technology, Schwarzenbergstraße 95c, 21073 Hamburg, {alireza.abedian;alexander.duester}@tuhh.de

Key words: Finite cell method, Fictitious domain method, Abaqus user element subroutine (UEL), Porosity.

ABSTRACT

In the paper at hand we introduce the basic concept for an adaptation and implementation of the finite cell method (FCM) within the commercial software ABAQUS$^{\text{TM}}$. Our goal is to analyse the influence of gas pores in aluminum die cast components on their strength and life span. Pores are technological unavoidable in the aluminium die cast process, cf. Fig. 1. The recently developed FCM is a straightforward combination of the standard finite element (FE) technology and the fictitious domain concept (FDC) [6], where the porous micro-structure can be taken into

Figure 1: Cast part including micro-structural details in the simulation [2].

consideration as STL[1] file (STL is the standard tessellation language) obtained from computed

[1]The STL format is frequently applied in rapid prototyping and it is used to interact with stereo-lithography machines.

tomography (CT) scans [5]. In applying the usual FE-based approach also the porous microstructure has to be discretized using geometry-conforming finite elements. However, this would result in models with a high number of finite elements which cannot be analyzed in a timely manner. The outstanding advantage of FDCs, such as the FCM, is to avoid body fitted meshes. Its basic idea is to embed the geometrically complex structure into an embedding domain such that their union yields an extended domain of simple shape which is automatically discretized deploying a non-conformal discretization. The physical geometry of the structure under investigation is only taken into consideration during the calculation of the stiffness matrices by an adaptive composed quadrature rule or another specifically tailored integration procedure [4]. Although the discretization does not conform to the physical boundary of the domain high-fidelity results are recovered if the numerical integration is accurate enough [1].
With regard to practical applications we are convinced that a robust implementation of the fictitious domain methodology within a wide-spread and established software tool like Abaqus would create a higher applicability of this method to complex engineering problems. Here, our specific focus is on the analysis of the influence of the porosity on the strength and the life span of die cast components. To this end, we developed a user subroutine (UEL) that is able to incorporate the required functionality. The implementation is based on standard hexahedral,

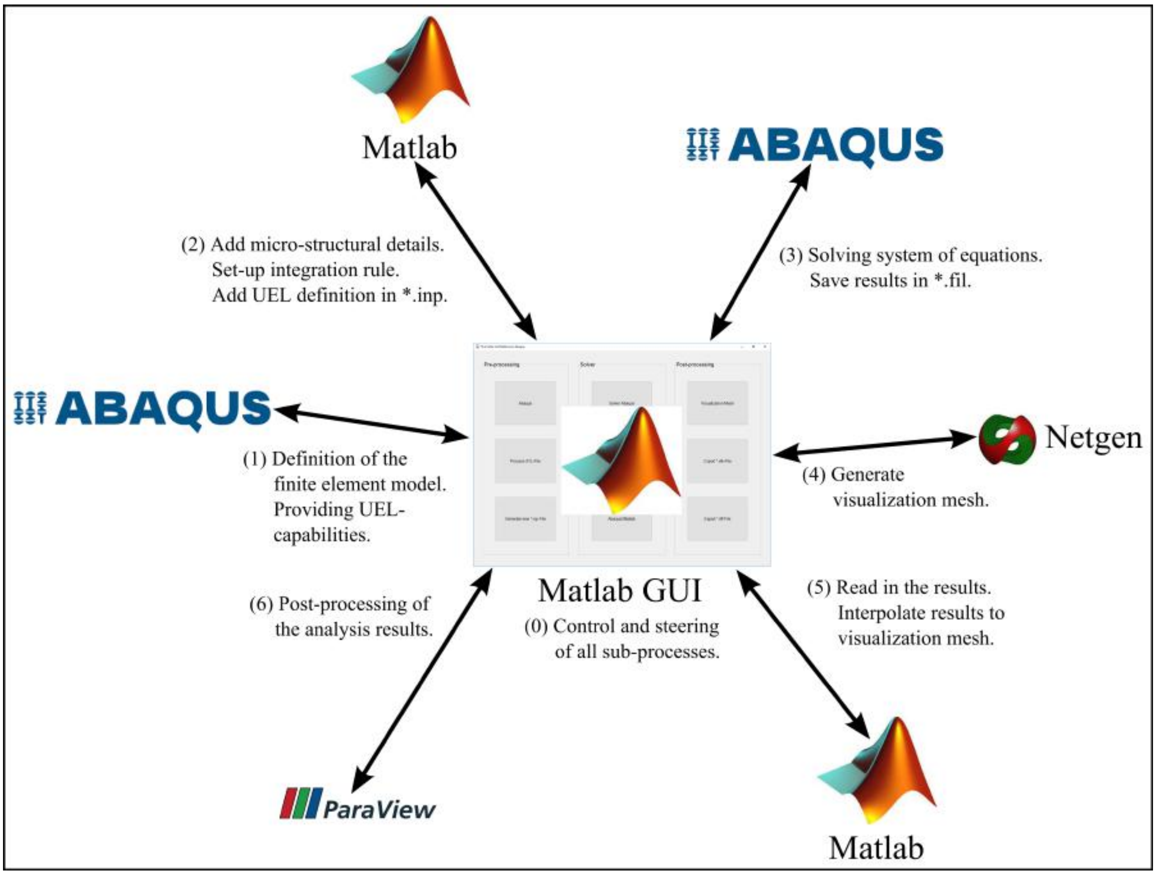

Figure 2: Workflow of the Abaqus FCM implementation.

pentahedral and tetrahedral finite elements [3]. Both details concerning the required input data and the necessary pre- as well as post-processing tools – although not directly related to Abaqus

– are provided. Besides pores obtained from CT measurements also artificial (virtual) discontinuities can be taken into account in the design process. Thus, the topology of the component can be optimized with respect to the technological requirements of the die casting production.
The whole workflow of our implementation including the pre- and post-processing stages is illustrated in Fig. 2. The initial model is set up in the pre-processing module of Abaqus. Here, the material properties and the element type is defined. In the next step an Abaqus input file is generated. This file is further processed in Matlab and adjusted to incorporate the user defined element routine (UEL). At this stage the micro-structural details (obtained from CT scans) are added to the analysis and also the necessary details to perform the composed numerical integration are generated. During the solution of the governing equations these data are read in by the UEL. For a smooth post-processing a geometry-conforming visualization mesh is created. This can be achieved by using powerful external mesh generators such as Netgen [7]. The analysis results are accordingly interpolated onto the new visualization nodes using the finite element shape functions and saved in the vtk-file format. This format can be processed by free scientific visualization software ParaView, which offers all capabilities of commercial FE post-processing tools.
In the current paper the theoretical background and the implementation of the FCM within Abaqus are presented in detail. Finally, the application of the developed software extension is shown by means of several test problems and engineering applications.

ACKNOWLEDGEMENT
The project is financially supported by the European Regional Development Fund (ERDF) and the German State of Saxony-Anhalt. This support is gratefully acknowledged. The first author also gratefully acknowledges the support provided by the German Research Foundation (DFG) under grant DU 1613/1-1.

REFERENCES

[1] Dauge, M. and Düster, A. and Rank, E. Theoretical and Numerical Investigation of the Finite Cell Method. *J Sci Comput.* 62:222–227 (2015).

[2] Duczek, S. and Berger, H. and Ambos, E. and Gabbert, U. Eine neue Methode zur Berücksichtigung des Einflusses der Porosität in Al-Druckgussteilen auf die Festigkeit Ein Beitrag zum Leichtbau. *Giesserei-Rundschau.* 62:222–227 (2015).

[3] Duczek, S. and Duvigneau, F. and Gabbert, U. The Finite Cell Method for Tetrahedral Meshes. *Finite Elem Anal Des* . 121:18–32 (2016).

[4] Duczek, S. and Gabbert, U. Efficient Integration Method for Fictitious Domain Approaches. *Comput Mech.* 56:725–738 (2015).

[5] Düster, A. and Sehlhorst, H.-G. and Rank, E. Numerical Homogenization of Heterogeneous and Cellular Materials Utilizing the Finite Cell Method. *Comput Mech.* 50:413–431 (2012).

[6] Parvizian, J. and Düster, A. and Rank, E. Finite Cell Method: *h*- and *p*-Extension for Embedded Domain Problems in Solid Mechanics. *Comput Mech.* 41:121–133 (2007).

[7] Schöberl, J. NETGEN An Advancing Front 2D/3D-Mesh Generator Based on Abstract Rules. *Comput Visual Sci* . 1:41-52 (1997).

A holistic simulation workflow to design an acoustically optimized electric wheel hub motor

F. Duvigneau[1], S. Perekopskiy, R. Kasper, U. Gabbert

Institute of Mechanics & Institute of Mobile Systems
Universitaetsplatz 2, Otto von Guericke University, D-39106 Magdeburg, Germany

Abstract

In the paper a holistic simulation workflow is presented which enables the designer to analyze the acoustic behavior of electric wheel hub motors numerically. The applied electric wheel hub motor shows an extraordinary power-to-weight-ratio, as it combines two different types of winding to boost torque sharing the same magnetic circuit [1]. One is an air gap winding and the other one is a slot winding (see Fig. 1, first row, right). In the development process of an engine the acoustics is usually not in the focus of interest. But, it has been proved that the acoustic characteristic of electric engines is a very important topic which should be taken into account in an early stage of the development process. In contrast to combustion engines in electrical engines the first engine orders are related to much higher frequencies (up to 1250 Hz) and the resulting sound is not so noisy. It seems that the radiated sound is caused by a few different frequencies only, as the second and the third engine order are the most important engine orders beside the first order, but even their amplitudes are with about 5% and 2% of the first one comparably small. Hence, the emitted sound of an electric engine is more like a single high frequency tone. Unfortunately, the human auditory perception is very sensitive with respect to such high frequency sounds. Consequently, the noise emission of electric engines is more annoying than the noise emission of combustion engines, even if the amplitudes of the electric sound are lower. For this reason, it is important to consider the acoustic behavior as early as possible in the product development process of an electric engine.

With aid of an overall simulation workflow the acoustics of electric engines can be optimized before the first prototype has been built. The paper at hand presents the simulation workflow of an electric wheel hub motor, which allows the prediction of the acoustic behavior based on the CAD-geometry only. The workflow consists of three steps as shown in Fig. 1. First, the electromagnetic behavior is modeled, where it is common to neglect the differences in the direction of the rotation axis to increase the efficiency. It is sufficient two use a two dimensional model only (see Fig. 1, right upper corner), as the attenuation of the tangential magnetic forces is less than 5% at the boarders. Further, the magnetic forces in radial direction are non-linear and cause stability problems, if they will be linearized. Second, the electromagnetic forces as result of the first step are used to calculate the vibrational behavior of the wheel hub motor. Third, the resulting surface velocity is used to excite the surrounding air and to calculate the air pressure at any point of the surrounding air volume under free field conditions. The vibration and acoustic analyses can be solved in an uncoupled manner, as the feedback of the vibrating air on the much stiffer engine housing can be neglected. For all three solution steps, the electrodynamics, the structural dynamics and the acoustics the finite element method is used. In the vibration and acoustic

[1] Corresponding Author: Fabian Duvigneau, Phone: +49/391/67-52754, Fax: +49/391/67-12439, E-mail: fabian.duvigneau@ovgu.de

analyses tetrahedral elements with quadratic shape functions are used due to the complex geometry and the required accuracy which is tested by convergence studies. The acoustic simulations can be done with a much coarser mesh due to the larger wave length in the air. But, at the interface between the structure and the air volume it is appropriate to use a co-incident mesh, which is coarsened with increasing distance from the structure to reduce the computational effort of the approach. The developed and numerically tested overall work-flow is finally also validated by measurements.

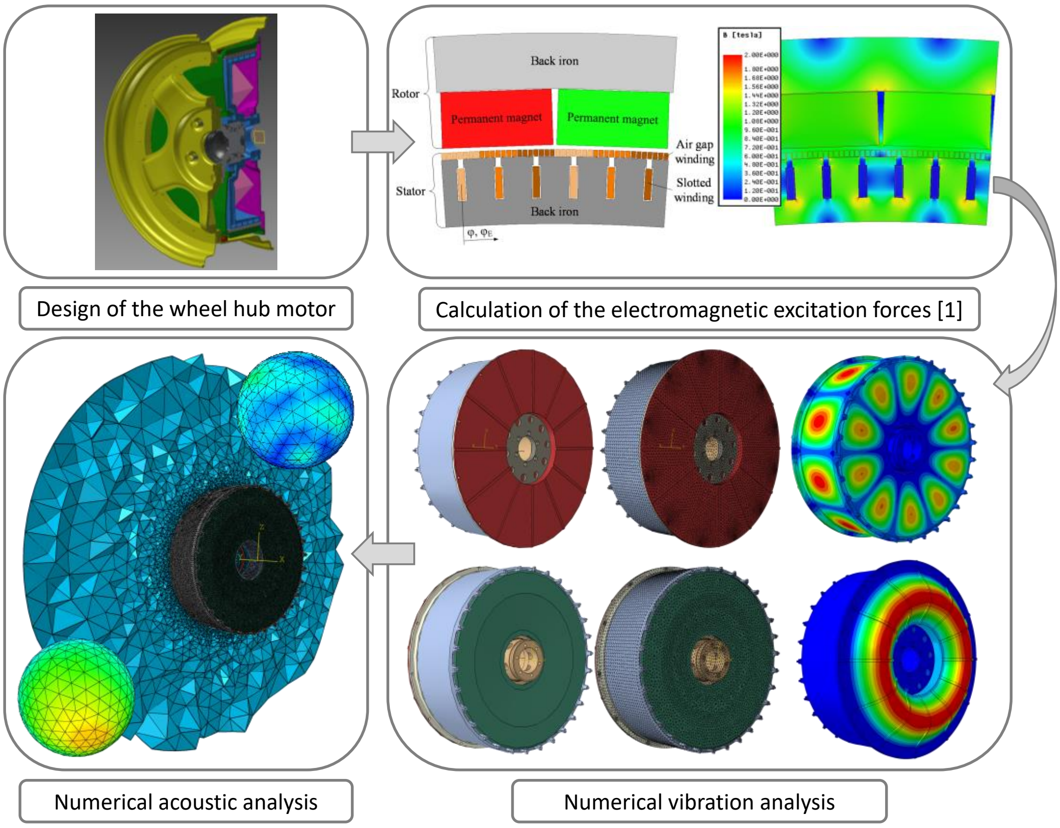

Figure 1: Holistic simulation workflow for calculating the sound radiation of an electric wheel hub motor based on the electromagnetic excitation forces

The presented overall virtual engineering methodology can be used to optimize the design of the wheel hub motor in further steps to fulfill it acoustic requirements. Furthermore, it would be a promising future development to extend the overall workflow by a psychoacoustic post-processing in order to include the special properties of human hearing sufficiently, instead of determining the classical acoustic parameter as sound pressure or power only [2].

References

[1] R. Kasper, N. Borchardt, Boosting Power Density of Electric Machines by Combining Two Different Winding Types, Proceedings of the 7th IFAC Symposium on Mechatronic Systems, Loughborough University, UK, September 5-8, 2016.

[2] F. Duvigneau, S. Liefold, M. Höchstetter, J. L. Verhey, U. Gabbert, Analysis of simulated engine sounds using a psychoacoustic model, Journal of Sound and Vibration, Volume 366, 2016, pp. 544-555. DOI: 10.1016/j.jsv.2015.11.034

Deformation Behavior of Hydrogel-layered PET Membranes

A. Ehrenhofer[1], **T. Wallmersperger**

Institut für Festkörpermechanik
George-Bähr-Str. 3c, TU Dresden, D-01069 Dresden, Germany

Abstract

Filtration membranes can be designed to allow controllable pore sizes with the help of smart hydrogels. In the current work, we present a composite system based on a PET membrane that is surface polymerized with the temperature-sensitive poly(N-isopropylacrylamide) (PNIPAAm) and patterned by laser-ablation. Simulation results of filtration and flow through the switchable membrane are presented. Then, the mechanical bending behavior of the actuated composite system and the weakening caused by the pores are investigated. Therefore, analytical mechanical investigations, as well as simulations performed by the Finite Element Method, are conducted. We show how the pore integration density can be optimized to reach high filtration performance without compromising the mechanical performance of the membrane.

1 Filtration through switchable pores

The separation of particle flows for analytical reasons can be realized by filtration using porous membranes [3]. The occurring process is size-exclusion due to contact of the particles and the membrane inside the pore (depth filtration) or for high particle loads in the filter-cake (surface filtration). For analytical processes e.g. in biological context, only low particle loads occur. Hence the membrane pore geometry is crucial for the filtration process.

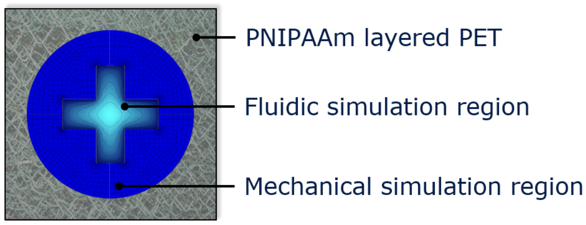

Figure 1: Structure of the membrane composite system.

In the present approach, we use a composite membrane structure comprising of a polyethylene terephtalate (PET) membrane backbone structure and a surface coating with a thermoresponsive poly(N-isopropylacrylamide) (PNIPAAm) hydrogel, see figure 1. Subsequent laser ablation of pore structures leads to controllable filtration properties in this system [1]. Since the geometrical shape of the pores is arbitrary, different pore-forms lead to different particle blocking and bypass behavior. A simple model for hydrogel swelling based on the similar thermal expansion leads to reasonable agreement with experimental observations.

[1]Corresponding Author: Adrian Ehrenhofer, Phone: +49/351/463-39171, Fax: +49/351/463-32450, E-mail: adrian.ehrenhofer@tu-dresden.de

2 Flow through the membrane

From simulations of the hydrogel swelling due to temperature stimulus, the evolution of pore opening in time can be predicted. Using (i) the theory of laminar flow in non-circular channels and (ii) the pore opening input, the flow through the pores was then simulated. The Poisson equation of Poiseuille flow $\nabla^2 v(x, y) = -K/\eta$ was used. Here, $v(x, y)$ denotes the fluid velocity that depends on the pressure gradient $K = dp/dz$; η is the dynamic viscosity of the fluid. We found out that in a limited range of opening and closing state of the valve, the drop in volume flux due to blocking can be used to evaluate the number of blocked pores in the membrane [2].

3 Mechanical theories for composite membrane bending

For the deployment of the system, a high number of pores is crucial. This is due to the fact that too few pores can lead to a clogging of the membrane resulting in unwanted surface filtration, i.e. the pores are no longer deciding for the filtration behavior. The predictability of the number of blocked pores from the integral volume flux is lost as well. In addition, with the higher number of pores, the membrane loses stiffness and reacts with a larger bending displacement under hydraulic pressure load. Different two-dimensional mechanical theories are applied and compared in order to quantify the influence of membrane bending to pore structure, see figure 2.

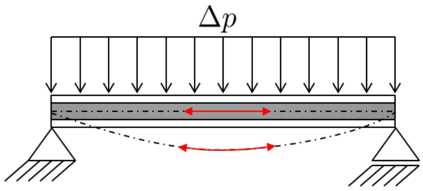

Figure 2: Large bending of the membrane due to uniform pressure load leads to a lengthening of the membrane and a subsequent shape change of the pores.

4 Conclusion

In the current work, we present the influence of increased pore integration density on the mechanical behavior of hydrogel composite membranes. When the number of pores increases, the hydraulic pressure load leads to large membrane deflection. This influences filtration performance unfavorably. An optimum for the number of pores can be found.

References

[1] Ehrenhofer, A.; Bingel, G.; Paschew, G.; Tietze, M.; Schröder, R.; Richter, A.; Wallmersperger, T. : Permeation Control in Hydrogel-Layered Patterned PET Membranes with Defined Switchable Pore Geometry - Experiments and Numerical Simulation. In: *Sensors and Actuators B: Chemical* 232 (2016), 499-505.

[2] Ehrenhofer, A.; Wallmersperger, T. : Adjustable Fluid and Particle Permeation through Hydrogel Composite Membranes. In: *Journal of Intelligent Material Systems and Structures* - under review

[3] Ulbricht, M. : Advanced functional polymer membranes. In: *Polymer* 47 (2006), Nr. 7, 2217 - 2262.

Analytical, Experimental and Numerical Analysis of Stability and Degradation of Smart Structure for Cubic Reconnaissance Satellites

H. Elahi[1], P. Gaudenzi[1], V. Cardini[1], M. Eugeni[1], G. Graterol Nisi[1], M. Pasquali[1], L. Pollice[1]

[1] Department of Mechanical and Aerospace Engineering, Sapienza University of Rome, Via Eudossiana 18, 00184, Rome Italy

Corresponding Author: hassanelahi_uet@yahoo.com

Abstract

Piezoelectric materials are widely used as smart structure in cubic reconnaissance satellites because of their sensing, actuating and energy harvesting abilities. In this research work analytical model is developed under specified mechanical thermal shocking conditions, a special circuit and apparatus is designed for experimentation which is based on inverse piezoelectric effect using equivalent circuit method to find the relationship between resistance and peak to peak voltage of Lead Zirconate Titanate (PZT-5A4E) for cubic reconnaissance satellites by shocking it at variable frequencies and at variable resistances under various mechanical thermal shocking conditions and numerical simulations are carried out at various mechanical loading to determine the accumulative effect of the specified conditions. This model provides novel mechanism for characterizing smart structures using stability and Mechanical Quality Factor is validated by Nyquist Theorem and RH Table. It was found that resonance frequency is most critical element for degradation of a smart structure but it can be prevented by adding resistance to the system by decade box. From experimentation and simulation the optimum resistance at variable frequency and temperature is predicted which has various applications in field of smart structures for cubic reconnaissance satellites. The response of the analytical calculations to the experimental and numerical calculations is within good agreement.

1 Introduction:

Satellites have been used for a number of military purposes, including infrared sensors that track missile launches; electronic sensors that eavesdrop on classified conversations; the future of Aerospace industry is dependent on smart structures [1]. These satellites need constant voltage power source for the actuation of these sensors [2]. Mechanical Quality Factor [3] of PZT plays a vital role for prediction of degradation of smart structure. The ultimate goal of this research paper is to use piezoelectric material as a smart structure for the construction of cubic reconnaissance satellite that can also be utilized as power source, wireless sensors and actuators, Structural Health Monitoring and prediction of Mechanical Quality Factor at a same time.

2 Research Methodology

In this research work, a translation model for smart structure cubic reconnaissance satellites was developed to predict the response of piezoelectric material under thermal shocking at various frequency and resistance conditions. Stability of the system is analyzed by Nyquist Theorem by plotting the poles and zeros via RH method. A specially designed setup is designed on basis of inverse piezoelectricity. Simulations are performed in ABAQUS.

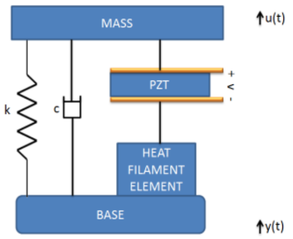

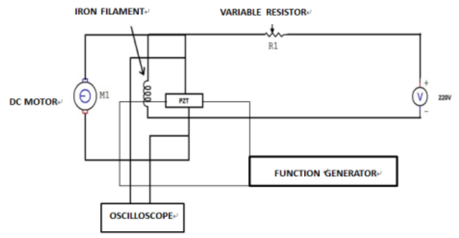

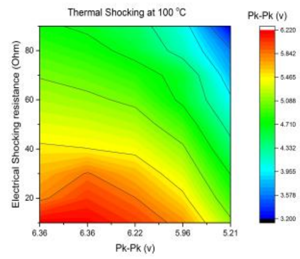

Fig. (a) Analytical Model Fig. (b) Circuit Diagram Fig. (c) Simulation

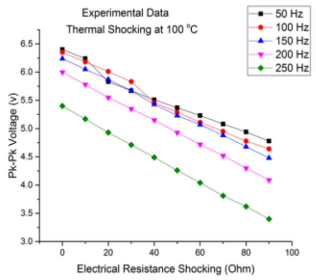

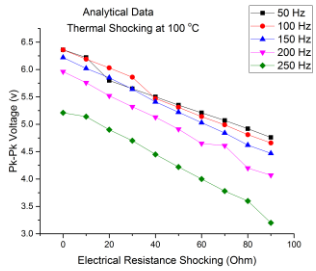

Fig. (d) Experimental Data Fig. (e) Analytical Data

3 Conclusion

In this research work, a single degree of freedom analytical model is developed which is verified by numerical as well as by experimentation. Following conclusions are made on the basis of analytical, experimental and numerical solution:

1. Characterization of smart structures for CubeSat is mainly dependent on Mechanical Quality Factor of Piezoelectric i.e., Degradation of a smart structure is directly proportional to Mechanical Quality Factor.
2. Thermal Shocking has a deep impact on polarization effect of piezoelectric material as it effect generation of $V_{pk\text{-}pk}$ exponentially.
3. The overall system showed stability as all the poles and zeros lie on left side of plane and the rate of degradation can be predicted anytime by the location of poles.
4. Resonant frequency and resistance have inverse relationship to $V_{pk\text{-}pk}$ and Mechanical Quality Factor as well but still they are required to characterized and stabilize the poling effect in inverse piezoelectricity method by restricting the freely intermolecular movement.

References

[1] Noor, A.K., et al., Structures technology for future aerospace systems. Computers & Structures, 2000. 74(5): p. 507-519

[2] Z. Butt, R.A. Pasha, F. Qayyum, Z. Anjum N. Ahmad, H. Elahi (2016) ―Generation of Electrical Energy using Lead Zirconate Titanate (PZT-5A) Piezoelectric Material: Analytical, Numerical and Experimental Verifications‖, Journal of Mechanical Science and Technology, Volume No. 30, pp. 3553-3558, 2016

[3] H. Elahi, R. A. Pasha and M. Z. Khan, (2014), Experimental Determination of Mechanical Quality Factor of Lead Zirconate Titanate (PZT-5A4E) by Equivalent Circuit Method under various Thermal and Resistance Conditions‖. Technical Journal, University of Engineering and Technology Taxila, pp 1-4, 2014.

Structural health monitoring (SHM) of safety-relevant lightweight structures using ultrasonic guided waves

Ulrich Gabbert, Sascha Duczek

Institute of Mechanics, Otto-von-Guericke-University of Magdeburg,
Universitaetsplatz 2, D-39106 Magdeburg, Germany

Abstract

Safety-relevant structures have to be permanently monitored to guarantee their integrity and functionality at all times. Therefore, the development of new monitoring strategies is currently a very active research field [1]. Especially the monitoring of modern lightweight constructions made of carbon and glass fiber-reinforced plastics (CFRP/GFRP) receives growing interest, especially from the aeronautics industries, but, also from producers of wind power plants, cars, ships and others. Especially impacts at carbon and glass fiber reinforced composites may cause damages which cannot be recognized by visual inspections, so called barely visible impact damage (BVID). Such damages can grow step by step during operation and may cause extreme accidents if they are not detected in time (see Fig. 1).

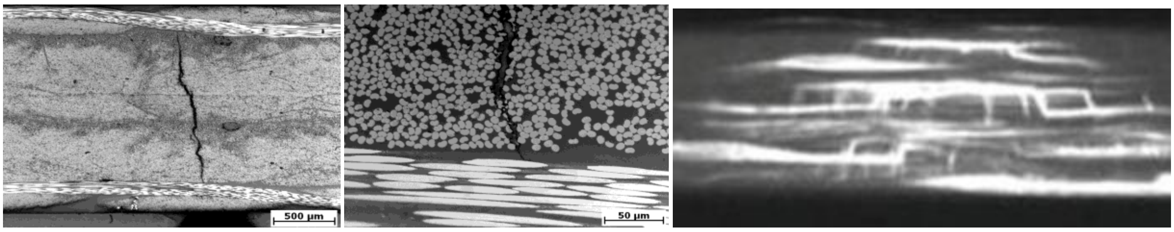

Figure 1: X-ray images of damages in cross sections of carbon reinforced composites after impacts [8]

Due to the danger of such invisible damages an integrated monitoring of such structures is of great significance. One of the most promising methods for enabling the development of powerful structural health monitoring (SHM) systems is based on ultrasonic guided waves, commonly referred to as Lamb waves. Comprehensive investigations and studies have shown that induced ultrasonic elastic waves in thin-walled structures can travel over long distances and show a high sensitivity with respect to damages. Lamb wave based methods take advantage of mode conversions and wave reflections at discontinuities, which can be used to identify structural damage, such as cracks, delaminations and others. Lamb waves can be simply excited and measured by a network of thin piezoelectric transducers glued to or integrated into the structure. The high sensitivity of Lamb waves with respect to small structural changes and the low costs of a network built from piezoelectric patches, make such SHM systems very attractive for industrial applications. Over the last decade the research activities in the field of SHM have been growing steadily (e.g. [2], [3], [4]). But, unfortunately, there are a lot of open questions, especially regarding the application of Lamb waves in layered composite structures and heterogeneous materials, such as sandwich materials with core layers made of honeycomb structures, hollow spheres or foam type materials.

In the first part of the presentation an overview about the outcome of an interdisciplinary research project regarding the development of SHM systems is given (Fig. 2). The project was financially supported by the German Research Foundation (DFG) and undertaken by researchers from the Universities of Magdeburg, Brunswick and Hamburg and the German Aerospace Center in Brunswick. The main results of this project have been collected in Springer a book, which will appear in 2017 [8]. In the presentation experimental approaches as well as numerical methods are discussed.

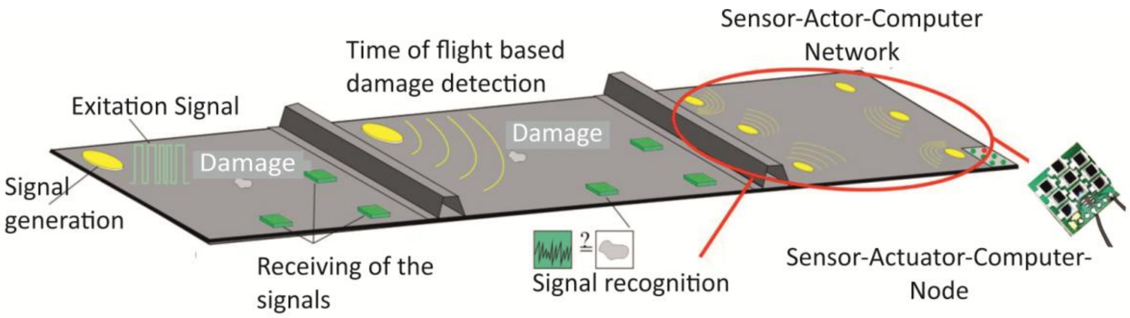

Figure 2: Methodology of an ultrasonic based structural health monitoring system [7]

In the second part an insight in efficient numerical approaches to simulate the propagation of ultrasonic waves and its interaction with damages in thin-walled composite structures and sandwich structures with heterogeneous core layers, such as honeycomb, hollow spheres etc., is demonstrated [5], [6], [7].

The advantage of higher order finite element schemas regarding their accuracy, convergence behavior and efficiency is shown [5] and the application for SHM purposes is exemplarily demonstrated (Fig. 3). Moreover, it is shown that the finite cell method (FCM) which is a straight forward combination of higher order FEM and fictitious domain methods is of great advantageous for wave propagation analysis in structures made from cellular materials [7], [8]. Especially the meshing is simplified, because the method avoids body-fitted discretizations. The microstructure can be taken into account by data obtained from computed tomography scans.

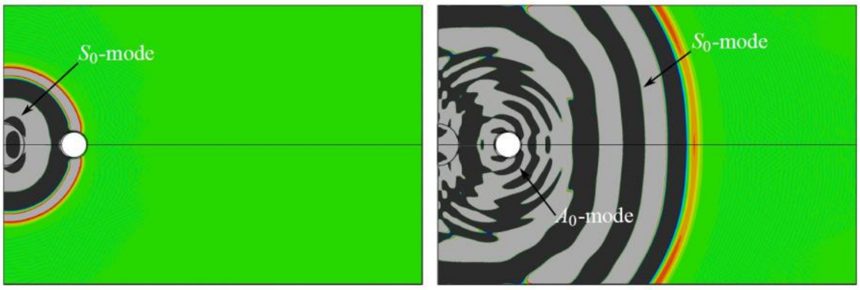

Figure 3: Simulation results showing the contour plot of the displacement perpendicular to a plate with a circular damage at two different time steps; the incident symmetric S_0-wave packet (left) interacts with the damage such resulting in a partial mode conversion to the anti-symmetric A_0-mode (right) [8]

ACKNOWLEDGEMENT: The project has been financially supported by the German Research Foundation (DFG) under the project numbers GA 480/13-(1-3). This support is gratefully acknowledged.

Literature

[1] Balageas D, Fritzen C P, Alfredo Guemes (Editors) (2006) *Structural Health Monitoring*, Iste Publishing Company.

[2] Gopalakrishnan S, Ruzzene M, Hanagud S (2011) *Computational Techniques for Structural Health Monitoring* (Springer Series in Reliability Engineering) Springer London.

[3] Ostachowicz W, Kudela P, Krawczuk M, Zak A (2012) *Guided Waves in Structures for SHM* J Wiley & Sons.

[4] Giurgiutiu V (2014) Structural Health Monitoring with Piezoelectric Wafer Active Sensors, Academic Press

[5] Willberg, C., Duczek, S., Vivar-Perez, J. M., Schmicker, D., Gabbert, U.: Comparison of different higher order finite element schemas for the simulation of Lamb waves, *Comput. Methods Appl. Mech. Engrg.*, 241-244 (2012), pp. 246-261.

[6] Hosseini, S.M.H., Duczek, S., Gabbert, U.: Damage localization in plates using mode conversion characteristics of ultrasonic guided waves, *Journal of Nondestructive Evaluation*, March 2014, Volume 33, Issue 1, pp 152-165.

[7] Duczek, S., Joulaian, M., Düster, A., Gabbert, U. (2014): Numerical analysis of Lamb waves using the finite and spectral cell methods, *Int. J. for Numer. Meth. in Engng*. 2014; 99:26–53.

[8] Lammering, R., Gabbert, U., Sinapius, M., Schuster, T. (Eds.) (2017): *Lamb-Wave Based Structural Health Monitoring in Polymer Composites*, Springer (in print).

Tensor nonlinear materials: potentiality and establishing experiments

D.V. Georgievskii*

Lomonosov Moscow State University, Leninskie Gory, 1, Moscow 119991, Russia

Abstract

Isotropic quadratic nonlinear tensor-functions modeling in the theory of constitutive relations a kind of materials where effects of second order, in particular, non-coaxiality of kinematic and stress tensors, have place, are considered. The tensor functions having a scalar potential and connecting two symmetric deviators of the second rank are of interest. In this case the conditions of potentiality have been integrated. It is shown that the first integral involves two arbitrary functions of quadratic invariant of the tensor-argument and one arbitrary function of its cubic invariant. Tensor nonlinear generalization of rigid viscoplastic model (two constant Bingham solid) is realized [1].

A principal scheme of the establishing experiments for finding three material functions of tensor nonlinear constitutive relations in continuum mechanics is described. These material functions are the functions of three invariants of stress state. It is proposed to use the long cylindric hollow rods for which one can effect any combination of the following realizable in experiments basic stress states: uniaxial extension, torsion, longitudinal shear, compression [2].

References

[1] D.V. Georgievskii, Potentiality of isotropic nonlinear tensor functions relating two deviators, Mechanics of Solids, 2016, vol. 51, no. 5, pp. 619-622.

[2] D.V. Georgievskii, Establishing experiments in tensor nonlinear theories of continuum mechanics, Moscow University Mechanics Bulletin, 2016, vol. 71, no. 2, pp. 49-50.

* D.V. Georgievskii, , e-mail: georgiev@mech.math.msu.su

A hygro-thermal stress finite element analysis of laminated beam structures by hierarchical one-dimensional modelling

Y. Hui, G. Giunta, S. Belouettar, E. Carrera and H. Hu

Abstract Composite structure operating under severe temperature conditions and/or wet environments are very common is several engineering fields such as aeronautics, space and transportation.
Hygro-thermal solicitation of beam-like structures results in a three-dimensional response that classical one-dimensional models are not always capable of describe effectively. An accurate prediction calls, then, for refined higher-order theories making this subject of research relevant and up-to-date.
In this work, laminated composite three-dimensional beams subjected to thermal and hygroscopic stresses are analysed. Several beam models are hierarchically derived by means of a unified formulation [1, 2] that allows for a theoretical derivation of the finite elements independent from the displacements polynomial approximation order over the cross-section as well as the number of nodes per element. Elements stiffness matrix are derived in a compact form ("fundamental nucleus") via the Principle of Virtual Displacements. As a result, a family of several one-dimensional finite elements accounting for transverse shear deformations and cross-section in- and out-of-plane warping can be obtained. Temperature and humidity profiles are obtained by directly solving the corresponding diffusion equation (Fourier's heat conduction equation for temperature and Fick's law for moisture).

Yanchuan Hui
Luxembourg Institute of Science and Technology, Politecnico di Torino, Wuhan University, e-mail: yanchuan.hui@list.lu

Gaetano Giunta
Luxembourg Institute of Science and Technology, e-mail: gaetano.giunta@list.lu

Salim Belouettar
Luxembourg Institute of Science and Technology, e-mail: salim.belouettar@list.lu

Erasmo Carrera
Politecnico di Torino, e-mail: erasmo.carrera@polito.it

Heng Hu
Wuhan University, e-mail: huheng@whu.edu.cn

These fields are, then, accounted as sources terms in the elastic analysis through Hooke's law.
Simply supported and cantilever configurations are considered. Numerical results in terms of temperature, moisture, displacement and stress distributions are provided for different beam slenderness ratios. Three-dimensional finite element solutions developed within the commercial code Ansys are presented for validation. The numerical investigations show that the hygro-thermo-elastic problem presents a complex three-dimensional stress state that can be efficiently obtained by a suitable choice of approximation order over the cross section: the accuracy is comparable to the reference solutions whereas the computational costs can be considerably reduced.

References

1. Carrera, E.: Theories and finite elements for multilayered plates and shells: a unified compact formulation with numerical assessment and benchmarking. Archives of Computational Methods in Engineering **10**, 215–296 (2003)
2. Carrera, E., Giunta, G., Petrolo, M.: Beam Structures: Classical and Advanced Theories. Wiley-Blackwell, UK (2011)

Investigation of the production and dissipation of heat on dynamically driven Dielectric Elastomer Actuators

Mario Kleo[1], Thomas Wallmersperger

Institut für Festkörpermechanik, Technische Universität Dresden
George-Bähr-Str. 3c, D-01069 Dresden, Germany

Abstract

Dielectric Elastomers (DEs) are smart materials and belong to the class of electric Electroactive Polymers (EAP) [1]. They are constructed as thin dielectric polymer layers, which are coated with compliant electrode layers. An applied electric potential difference between the electrodes leads to an electrostatic force and as consequence to a deformation of the Dielectric Elastomer Actuator (DEA) in thickness direction. To achieve larger absolute displacements, DE-based actuators are built as stacks from multiple layers of single DE elements [2]. The crucial properties of DEA are the permittivity of the dielectric material and the elasticity of the whole structure. In the present research a modeling approach of the thermal behavior of DEAs is proposed and investigated in detail.

1 Introduction

As Dielectric-Elastomer applications subjected to changing loads of high frequency lead to a heating of the structure, the dynamic behavior of Dielectric Elastomers can only completely be described by also considering the thermal field. In order to simulate the dynamic operations, the reasons for heat production and dissipation have to be considered, both (i) for delivering boundary conditions for temperature-dependent mechanical and electrical material properties or (ii) for avoiding damage.

2 Modeling of the thermal bahavior fo DEAs

In this work the effects of different causes for heating and cooling will be investigated as depicted in Fig. 1. The major effects on the thermal field of dynamically driven DEs are (i) the convective cooling, (ii) the resistive heating and (iii) the viscoelastic heating. The convective cooling, which is assumed to be a free convection, is dependent on the difference in temperature of the outer shell of the DE and the surrounding medium. The resistive heating occurs due to the Ohmic resistance of the electrode during the charge and discharge process. Since this resistance is dependent of the material and the geometry of the electrode, an approach in the framework of electrostatics in continua is used in order to simulate the transient process of varying voltages. As consequence of the viscous material property the dynamic movement leads to a viscous loss and thus also to a heating. The viscoelastic mechanical behavior is considered by a hyperelastic material approach. This

[1]Corresponding Author: Mario Kleo, Phone: +49 351 463-39659, Fax: +49 351 463-32450, E-mail: Mario.Kleo@tu-dresden.de

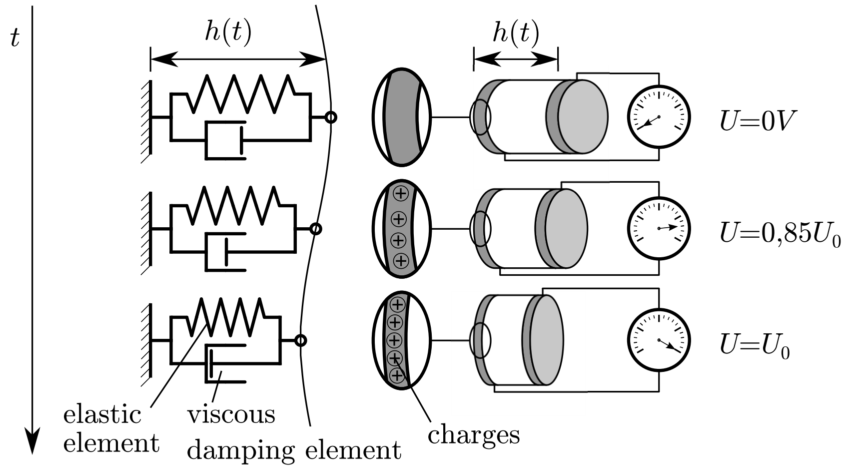

Figure 1: Major effects of heating in dynamically driven Dielectric Elastomer Actuators; change of thickness h in dependency of time t

approach is based on Ogden [3] and extended by using a Prony-series description [4] for the viscous part. In the present research, these mechanisms will be investigated in detail. First, these effects are modeled in order to later incorporate them into a coupled thermo-electro-mechanical formulation. Depending on the frequency and the type of the load, viscoelastic and resistive heating have a different contribution during the dynamic deformation process. In the present investigation, a numerical study will consider both electrical and mechanical loads.

3 Conclusion and Outlook

In the present work, a modeling apporach is proposed and investigated in detail, in order to provide a simulation method to quantify the major effects on the thermal field in Dielectric Elastomer Actuators. The results of this investigation are intended to be used to create a coupled thermo-electro-mechanical formulation for dynamically driven Dielectric Elastomer Actuators.

References

[1] Yoseph Bar-Cohen. Electroactive polymers as artificial muscles - reality and challenges. *Jet Propulsion Laboratory Technical Report Server 1992+*, 04, 2001.

[2] Henry Haus, Marc Matysek, Holger Mößinger, and Helmut F Schlaak. Modelling and characterization of dielectric elastomer stack actuators. *Smart Materials and Structures*, 22(10):104009, 2013.

[3] Raymond William Ogden. Large Deformation Isotropic Elasticity - On the Correlation of Theory and Experiment for Incompressible Rubberlike Solids. *Proceedings of the Royal Society of London. A. Mathematical and Physical Sciences*, 326(1567):565–584, 1972.

[4] Michael Wissler and Edoardo Mazza. Modeling and simulation of dielectric elastomer actuators. *Smart Materials and Structures*, 14(6):1396–1402, 2005.

Strong and weak sampling surfaces formulations for 3D stress and vibration analyses of layered piezoelectric plates

G. M. Kulikov[*], S.V. Plotnikova

Laboratory of Intelligent Materials and Structures
Tambov State Technical University, Sovetskaya, 106, Tambov 392000, Russia

Abstract

This paper focuses on implementation of the sampling surfaces (SaS) method [1] for the three-dimensional (3D) stress and vibration analyses of layered piezoelectric plates. The SaS formulation is based on choosing inside the layers the arbitrary number of not equally spaced SaS parallel to the middle surface in order to introduce the displacements and electric potentials of these surfaces as basic plate unknowns. Such choice of unknowns permits the presentation of the proposed piezoelectric plate formulation in a very compact form. The SaS are located inside each layer at Chebyshev polynomial nodes that improves the convergence of the SaS method significantly. Therefore, the SaS formulation can be applied efficiently to analytical solutions for layered piezoelectric plates, which asymptotically approach the 3D exact solutions of electroelasticity as the number of SaS tends to infinity. The strong SaS formulation is based on integrating the equilibrium equations of piezoelectricity, whereas the weak SaS formulation is based on a variational approach proposed earlier by the author [2].

1 Variational SaS formulation

Consider a layered piezoelectric plate of the thickness h. Let the middle surface Ω be described by Cartesian coordinates x_1 and x_2. The coordinate x_3 is oriented in the thickness direction. According to the SaS concept, we choose inside the nth layer I_n SaS $\Omega^{(n)1}, \Omega^{(n)2}, ..., \Omega^{(n)I_n}$ parallel to the middle surface. The transverse coordinates of SaS of the nth layer located at Chebyshev polynomial nodes are written as

$$x_3^{(n)i_n} = \frac{1}{2}(x_3^{[n-1]} + x_3^{[n]}) - \frac{1}{2} h_n \cos\left(\pi \frac{2i_n - 1}{2I_n}\right), \tag{1}$$

where $x_3^{[n-1]}$ and $x_3^{[n]}$ are the transverse coordinates of interfaces $\Omega^{[n-1]}$ and $\Omega^{[n]}$; $h_n = x_3^{[n]} - x_3^{[n-1]}$ is the thickness of the nth layer; the index $n = 1, 2, ..., N$ identifies the belonging of any quantity to the nth layer, where N is the number of layers; the index $i_n = 1, 2, ..., I_n$ identifies the belonging of any quantity to the SaS of the nth layer.

The through-the-thickness SaS approximations can be expressed as

$$[u_i^{(n)}\ \varepsilon_{ij}^{(n)}\ \sigma_{ij}^{(n)}\ \varphi^{(n)}\ E_i^{(n)}\ D_i^{(n)}] = \sum_{i_n} L^{(n)i_n} [u_i^{(n)i_n}\ \varepsilon_{ij}^{(n)i_n}\ \sigma_{ij}^{(n)i_n}\ \varphi^{(n)i_n}\ E_i^{(n)i_n}\ D_i^{(n)i_n}], \tag{2}$$

where $u_i^{(n)}, \varepsilon_{ij}^{(n)}, \sigma_{ij}^{(n)}, \varphi^{(n)}, E_i^{(n)}, D_i^{(n)}$ are the displacements, strains, stresses, electric

[*]Corresponding author: G. M. Kulikov, e-mail: gmkulikov@mail.ru

potential, electric field and electric displacements of the *n*th layer; $u_i^{(n)i_n}$, $\varepsilon_{ij}^{(n)i_n}$, $\sigma_{ij}^{(n)i_n}$, $\varphi^{(n)i_n}$, $E_i^{(n)i_n}$, $D_i^{(n)i_n}$ are the displacements, strains, stresses, electric potential, electric field and electric displacements of SaS of the *n*th layer $\Omega^{(n)i_n}$; $L^{(n)i_n}(x_3)$ are the Lagrange basis polynomials of degree $I_n - 1$ corresponding to the *n*th layer:

$$L^{(n)i_n} = \prod_{j_n \neq i_n} \frac{x_3 - x_3^{(n)j_n}}{x_3^{(n)i_n} - x_3^{(n)j_n}} \quad (i_n, j_n = 1, 2, ..., I_n). \tag{3}$$

The variational SaS formulation for the laminated piezoelectric plate is based on a variational equation

$$\delta \iint_{\Omega} \sum_n \int_{x_3^{[n-1]}}^{x_3^{[n]}} \frac{1}{2}\left(\sigma_{ij}^{(n)}\varepsilon_{ij}^{(n)} - D_i^{(n)}E_i^{(n)}\right) dx_1 dx_2 dx_3 = \delta W, \tag{4}$$

where W is the work done by external electromechanical loads. Here, the summation on repeated Latin indices is implied.

2 Strong SaS formulation

For simplicity, we consider the case of linear piezoelectric materials given by

$$\sigma_{ij}^{(n)} = C_{ijkl}^{(n)}\varepsilon_{kl}^{(n)} - e_{kij}^{(n)}E_k^{(n)}, \quad D_i^{(n)} = e_{ikl}^{(n)}\varepsilon_{kl}^{(n)} + \in_{ik}^{(n)} E_k^{(n)}, \tag{5}$$

where $C_{ijkl}^{(n)}$, $e_{kij}^{(n)}$ and $\in_{ik}^{(n)}$ are the elastic, piezoelectric and dielectric constants of the *n*th layer.

The equilibrium equations and charge equation of electrostatics in the absence of body forces and free charges can be written as

$$\sigma_{ij,j}^{(n)} = 0, \quad D_{i,i}^{(n)} = 0, \tag{6}$$

where the symbol $(\ldots)_{,i}$ stands for the partial derivatives with respect to coordinates x_i.

The boundary conditions on bottom and top surfaces are defined as

$$u_i^{(1)}(-h/2) = w_i^- \text{ or } \sigma_{i3}^{(1)}(-h/2) = p_i^-, \quad \varphi^{(1)}(-h/2) = \Phi^- \text{ or } D_3^{(1)}(-h/2) = Q^-, \tag{7}$$

$$u_i^{(N)}(h/2) = w_i^+ \text{ or } \sigma_{i3}^{(N)}(h/2) = p_i^+, \quad \varphi^{(N)}(h/2) = \Phi^+ \text{ or } D_3^{(N)}(h/2) = Q^+, \tag{8}$$

where $w_i^-, p_i^-, \Phi^-, Q^-$ and $w_i^+, p_i^+, \Phi^+, Q^+$ are the prescribed displacements, surface tractions, electric potentials and electric charges at the bottom and top surfaces.

The continuity conditions at interfaces are

$$u_i^{(m)}(x_3^{[m]}) = u_i^{(m+1)}(x_3^{[m]}), \quad \sigma_{i3}^{(m)}(x_3^{[m]}) = \sigma_{i3}^{(m+1)}(x_3^{[m]}),$$
$$\varphi^{(m)}(x_3^{[m]}) = \varphi^{(m+1)}(x_3^{[m]}), \quad D_3^{(m)}(x_3^{[m]}) = D_3^{(m+1)}(x_3^{[m]}), \tag{9}$$

where the index $m = 1, 2, ..., N-1$ identifies the belonging of any quantity to the interface $\Omega^{[m]}$.

Satisfying the equilibrium equations and charge equation at inner points $x_3^{(n)m_n}$ inside the layers, the following differential equations are obtained:

$$\sigma_{i1,1}^{(n)m_n} + \sigma_{i2,2}^{(n)m_n} + \sum_{i_n} M^{(n)i_n}(x_3^{(n)m_n})\sigma_{i3}^{(n)i_n} = 0, \tag{10}$$

$$D_{1,1}^{(n)m_n} + D_{2,2}^{(n)m_n} + \sum_{i_n} M^{(n)i_n}(x_3^{(n)m_n})D_3^{(n)i_n} = 0, \tag{11}$$

where $M^{(n)i_n} = L^{(n)i_n}_{,3}$ are the derivatives of the Lagrange basis polynomials whose values at SaS $\Omega^{(n)m_n}$ are evaluated in papers [1, 2] and $m_n = 2,3,...,I_n - 1$.

Next, we satisfy the boundary conditions

$$\sum_{i_1} L^{(1)i_1}(-h/2)u_i^{(1)i_1} = w_i^- \text{ or } \sum_{i_1} L^{(1)i_1}(-h/2)\sigma_{i3}^{(1)i_1} = p_i^-,$$
$$\sum_{i_1} L^{(1)i_1}(-h/2)\varphi^{(1)i_1} = \Phi^- \text{ or } \sum_{i_1} L^{(1)i_1}(-h/2)D_3^{(1)i_1} = Q^-, \tag{12}$$
$$\sum_{i_N} L^{(N)i_N}(h/2)u_i^{(N)i_N} = w_i^+ \text{ or } \sum_{i_N} L^{(N)i_N}(h/2)\sigma_{i3}^{(N)i_N} = p_i^+,$$
$$\sum_{i_N} L^{(N)i_N}(h/2)\varphi^{(1)i_N} = \Phi^+ \text{ or } \sum_{i_N} L^{(N)i_N}(h/2)D_3^{(N)i_N} = Q^+ \tag{13}$$

and the continuity conditions that result in

$$\sum_{i_m} L^{(m)i_m}(x_3^{[m]})u_i^{(m)i_m} = \sum_{i_{m+1}} L^{(m+1)i_{m+1}}(x_3^{[m]})u_i^{(m+1)i_{m+1}},$$
$$\sum_{i_m} L^{(m)i_m}(x_3^{[m]})\sigma_{i3}^{(m)i_m} = \sum_{i_{m+1}} L^{(m+1)i_{m+1}}(x_3^{[m]})\sigma_{i3}^{(m+1)i_{m+1}},$$
$$\sum_{i_m} L^{(m)i_m}(x_3^{[m]})\varphi^{(m)i_m} = \sum_{i_{m+1}} L^{(m+1)i_{m+1}}(x_3^{[m]})\varphi^{(m+1)i_{m+1}},$$
$$\sum_{i_m} L^{(m)i_m}(x_3^{[m]})D_3^{(m)i_m} = \sum_{i_{m+1}} L^{(m+1)i_{m+1}}(x_3^{[m]})D_3^{(m+1)i_{m+1}}. \tag{14}$$

Thus, the proposed strong SaS formulation deals with $4(I_1 + I_2 + ... + I_N)$ governing equations (10)-(14) for finding the same number of SaS displacements $u_i^{(n)i_n}$ and SaS electric potentials $\varphi^{(n)i_n}$. These differential and algebraic equations have to be solved to describe the response of the layered piezoelectric plate.

3 Benchmark problems

As numerical examples, we study the static and dynamic responses of simply supported laminated piezoelectric rectangular plates. The accuracy of both SaS plate formulations is compared with each other and the Heyliger's 3D exact solutions are adopted as benchmark solutions [3, 4].

References

[1] G.M. Kulikov, S.V. Plotnikova, Exact 3D stress analysis of laminated composite plates by sampling surfaces method, Compos. Struct., 2012, vol. 94, pp. 3654–3663.

[2] G.M. Kulikov, S.V. Plotnikova, Three-dimensional exact analysis of piezoelectric laminated plates via a sampling surfaces method, Int. J. Solids Struct., 2013, vol. 50, pp. 1916–1929.

[3] P. Heyliger, Exact solutions for simply supported laminated piezoelectric plates, J. Applied Mech., 1997, vol. 64, pp. 299–306.

[4] P. Heyliger, D.A. Saravanos, Exact free-vibration analysis of laminated plates with embedded piezoelectric layers, J. Acoustic Soc. Amer., 1995, vol. 98, pp. 1547–1557.

Robust CUF-based four-node and eight-node quadrilateral plate elements

T.H.C. Le, M. D'Ottavio, P. Vidal, O. Polit

Abstract In this work, a Finite Element (FE) implementation of variable-kinematics models based on Carrera's Unified Formulation (CUF) for composite plates using the commercial software Abaqus is presented. A new four-node and eight-node plate elements called QC4 and CL8, respectively, are proposed. These FE consider a specific approximation for the transverse shear strains on the basis of the 'field compatibility' paradigm with the aim of avoiding the transverse shear locking occurring in thin plates. Numerical assessments of the new FE are proposed with respect to some known pathologies of plate elements such as transverse shear locking, spurious zero energy modes and mesh distortion.

1 Introduction

The variable kinematics approach implemented in the framework of CUF allows the user to choose at runtime the plate model to be employed for the analysis. A large number of different plate models are formulated by selecting: (i) the variational formulation leading to the weak form, i.e., either the Principle of Virtual Displacement (PVD) or Reissner's Mixed Variational Theorem (RMVT); (ii) whether the variables are described in an Equivalent Single Layer (ESL) or Layer-Wise (LW) manner; ZigZag models can be formulated through the use of Murakami's ZigZag Function (MZZF); (iii) the order N of the polynomial approximation of the variable across the thickness of each layer (LW) or of the whole laminate (ESL) [1].

Variable-kinematics isoparametric PVD-based plate elements are known to suffer transverse shear locking, which has been contrasted by either reduced integration techniques or an extension of the MITC approach to the higher-order transverse shear strains [2]. In general, the transverse shear strains $\gamma_{\alpha 3}(x,y,z)$ $(\alpha = 1,2)$ can be split into a $z-$constant contribution $\gamma^0_{\alpha 3}(x,y)$ (independent of the thickness) and

e-mail: {thihuyencham.le, michele.d_ottavio, phillippe.vidal, olivier.polit}@u-paris10.fr
Laboratoire Energétique Mécanique Electromagnétisme, Univ Paris Nanterre, 50, Rue de Sèvres, 92410 Ville d'Avray, France

the $z-$dependent contributions $\gamma^{s}_{\alpha 3}(x,y,z)$ related to higher-order approximations. It is demonstrated that the locking pathology comes only from the $z-$constant terms $\gamma^{0}_{\alpha 3}(x,y)$. So, the aim of this study is to develop four-node and eight-node quadrilateral FEs upon extending to CUF the well-established QC4 and CL8 techniques originally formulated for FSDT plate elements [3] . The key idea is to use a dedicated interpolation of the $z-$independent transverse shear strains that is constructed in the natural reference frame on the basis of the field-consistency paradigm, which avoids the spurious locking constraint and provides an enhanced robustness with respect to mesh distortion.

The new quadrilateral four-node (QC4) and eight-node (CL8) variable-kinematics plate elements are all implemented within an Abaqus User Subroutine.

2 Numerical evaluations

An extensive numerical assessment of the new FEs is presented, which shows their accuracy, robustness and efficiency for thin to very thick multilayered composite plates. The performances in terms of convergence rate and accuracy on displacements and stresses are improved and numerical pathologies overcome. The eigenvalue analysis of the element stiffness matrix highlights the absence of spurious zero energy modes. Figure 1(a) exemplarily illustrates the shear locking correction and Figure 1(b) the robustness for distorted meshes (s measures the mesh distortion).

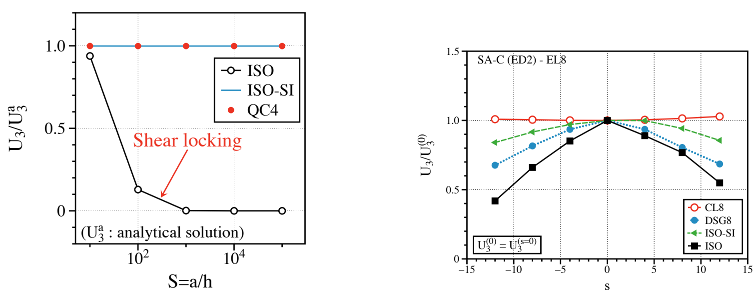

(a) Transverse shear locking

(b) Mesh distortion

Fig. 1: Some numerical results for the new QC4 and CL8 elements

References

1. E. Carrera, L. Demasi, Classical and advanced multilayered plate elements based upon PVD and RMVT. Part I. Derivation of finite element matrices, Int. J. Numer. Meth. Eng. vol. 55, pp. 191-231 (2002).
2. E. Carrera, M. Cinefra and P. Nali, MITC technique extended to variable kinematic multilayered plate elements, Compos. Struct. vol. 92, pp. 1888-1895 (2010).
3. O. Polit, M. Touratier and P. Lory, A new eight-node quadrilateral shear-bending plate finite element, Int. J. Numer. Meth. Eng. vol. 37, pp. 387-411 (1994).

Chemically induced swelling behavior of polyelectrolyte gels: Modeling and numerical simulation

P. Leichsenring[1], **T. Wallmersperger**

Institut für Festkörpermechanik
George-Bähr-Str. 3c, TU Dresden, D-01069 Dresden, Germany

Abstract

Polyelectrolyte gels are chemically synthesized materials with a distinct viscoelastic behavior. They comprise of a solid, fluid and ionic phase. Changing the ambient condition, e.g. a change in the ion concentration, triggers a certain equilibrium state which is governed by coupled fluid and ionic fluxes as well as by a mechanical stress. In order to homogenize the microstructure of the material a multiphase model based on the Theory of Porous Media is applied. With respective material laws, fluxes due to diffusion, migration and convection are considered. By performing numerical simulations, the time-dependent swelling behavior of polyelectrolyte gels is investigated for different mechanical constraints.

1 Continuum model

In the present work, a continuum model for polyelectrolyte gels is formulated. These materials consist of a solid phase and a fluid phase. Under deformation or after the application of external loads, these materials show a dominant viscoelastic behavior, which is in agreement to the gel-like properties. In addition, due to the presence of fixed charges, the fluid phase comprises mobile ions and therefore the distinct polyelectrolyte behavior can be depicted. As these type of materials is typically immersed in a solution bath the equilibrium state of polyelectrolyte materials also depends on the chemical composition of the surrounding solution.

The complex interaction of the constituents is captured by a statistical homogenization based on the Theory of Mixtures [1]. By incorporating the saturation condition, a representative volume element $\mathrm{d}v$ is defined by the superposition of the fluid phase {F} and the solid phase {S} as shown in Fig. 1:

$$\mathrm{d}v = \mathrm{d}v^{\mathrm{S}} + \mathrm{d}v^{\mathrm{F}} \ .$$

This definition – and a quantification based on the concept of volume fractions – is the fundamental concept of the Theory of Porous Media.

For each phase, the respective material laws are defined separately. For the solid phase, Hooke's law is prescribed. The fluid is assumed to have a constant viscosity. By incorporating further assumptions, the solid-fluid-interaction is then obtained by Darcy's law. The behavior of the ionic phase is described by a modified Nernst-Planck equation.

[1]Corresponding Author: Peter Leichsenring, Phone: +49 351 463 39171, Fax: +49 351 463 32450, e-mail: peter.leichsenring@tu-dresden.de

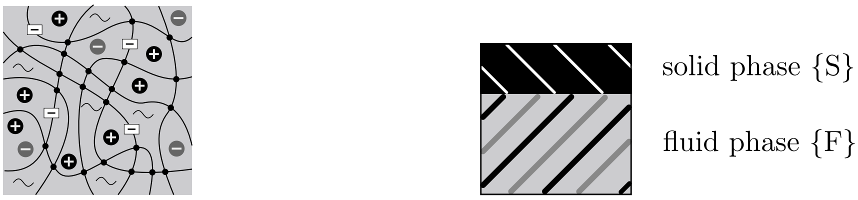

(a) Microscopic structure of the hydrogel with the incorporated constituents

(b) Homogenized structure of the hydrogel on the mesoscale

Figure 1: Hydrogel structure on the micro- and mesoscale

2 Numerical analysis

To investigate the coupled chemo-electro-mechanical behavior of polyelectrolyte gels, the derived field equations [2, 3] are solved in the framework of the Finite Element Method. The discretization in space is performed in two dimensions. For the fluid and ionic phase, a zero flux over the third dimension is assumed. The solid phase is considered in a plain strain configuration and in a plain stress configuration. The time discretization is performed by applying the implicit Euler scheme.

In a first study, the polyelectrolyte gel is stimulated by changing the ionic concentration in the surrounding solution bath. From respective jump conditions the chemical load is prescribed on the gel domain. Having investigated the free swelling behavior, in a second study, mechanical constraints are prescribed to analyze the hindered swelling behavior of polyelectrolyte gels. In order to validate the obtained results, a comparison with numerical results available in literature will be performed.

3 Conclusion and Outlook

In the present work, the coupled chemo-electro-mechanical swelling behavior of polyelectrolyte materials is numerically simulated. The obtained results lead to a more precise understanding of the chemo-electro-mechanical behavior of polyelectrolyte gels. By considering an external chemical stimulus, the material behavior is investigated for different mechanical constraints. From the obtained results, characteristic design guidelines of polyelectrolyte gels for actuator or sensor applications can be derived.

References

[1] R.M. Bowen, Theory of mixtures: in A.C. Eringen (Ed.), Continuum physics (Vol. III), Waltham: Academic Press, 1976

[2] P. Leichsenring, T. Wallmersperger, Modeling and simulation of transport phenomena in ionic gels: in Y. Bar-Cohen (Ed.), Proc. SPIE 9430, Electroactive Polymer Actuators and Devices (EAPAD), 2015, 94301I

[3] J. Bluhm, S. Serdas & J. Schröder, Theoretical framework of modeling of ionic EAPs within the Theory of Porous Media, Archive of Applied Mechanics. Vol. 86, 2016, pp. 3–19

MULTIOBJECTIVE OPTIMIZATION FOR ACTIVE VIBRATION ATTENUATION IN LAMINATED COMPOSITE PANELS

Ndilokelwa F. Luis(1), **J.F.A. Madeira**(1,2), **A. L. Araújo**(1), **A.J.M. Ferreira**(3)

(1)IDMEC, Instituto Superior Técnico, Universidade de Lisboa, Portugal
(2)ISEL, Instituto Superior de Engenharia de Lisboa, Portugal
(3)DEMEGI, Faculdade de Engenharia, Universidade do Porto, Portugal

Abstract

In the last decades, laminated composite structures have been widely used in aeronautic and aerospace applications. Normally, applications with composite structures in the aerospace field consist of large and lightweight panels, which are prone to vibration problems. The use of both passive and active treatments for structural energy dissipation is an efficient way of reducing vibration levels in lightweight structures. Passive treatments are achieved by incorporating viscoelastic materials in the structure and are suitable for high frequency damping, while active treatments with surface bonded piezoelectric patches are suitable for low frequency damping.

The main disadvantage of these passive and active treatments is precisely the increase in weight, as a result of the inclusion of the viscoelastic and piezoelectric materials. Optimization techniques play an important role in minimizing this unavoidable weight increase as they can obtain the best distribution of these materials in a given structure to ensure a good damping performance and, at the same time, adding the minimum mass to realize efficient treatments.

In this work, recent developments in vibration attenuation with active damping are introduced, showing the importance of an appropriate finite element model associated to a multiobjective optimization method. A finite element model based on the Carrera's Unified Formulation [1] was used, with a layerwise approach, for modeling and dynamic analysis of orthotropic plates with viscoelastic layer and piezoelectric layers or patches. A recent methodology of optimization, based on direct search techniques, was used: Direct MultiSearch (DMS) optimization. This methodology does not use derivatives and does not aggregate any of the problem objective functions. To the authors knowledge, it is the first time that DMS is applied to this class of problem where the number of patches is also a design variable. It has been applied previously to active damping design of sandwich structures [2] but with a fixed number of patches.

Multiobjective constrained optimization is conducted to determine optimal distributions of piezoelectric patches on the top and bottom surfaces of laminated plates with viscoelastic layers. The design variables are the number and position of these patches (Figure 1), and the objectives are the minimization of the number of patches, the maximization of the fundamental modal loss factor and the maximization of the fundamental natural frequency. In Table 1 an example of collocated patch distribution is shown for a simply supported laminated sandwich plate, where the difference between considering or not the eqipotential conditions on the electrodes is shown. In the paper, trade-off Pareto optimal fronts and the respective optimal active patch configurations are obtained and the results will presented, analyzed and discussed.

Acknowledgments

Ndilokelwa F. Luis would like to acknowledge the FCT, Fundação para a Ciência e Tecnologia, Portugal, for the financial support through grant SFRH/BD/77637/2011.

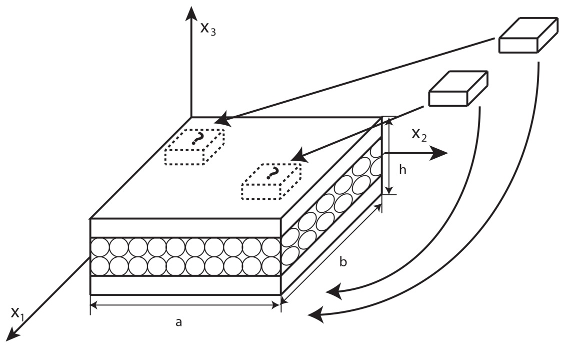

Figure 1: Hypothetical positioning of patches on a sandwich plate

Solution	A_2	B_2	C_2	D_2	E_2	F_2	G_2
Configuration	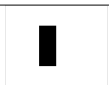		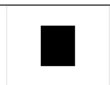	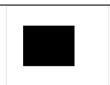		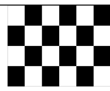	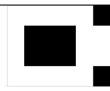
No. of patches	2	3	4	6	8	12	8
η_1 [%]	1.96	4.08	9.84	12.15	17.60	23.87	12.52
f_1 [Hz]	208.15	209.21	213.61	214.21	215.17	204.04	215.91
Solution	H_2	I_2	J_2	N_2	K_2	L_2	M_2
Configuration	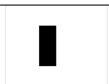	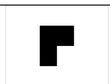	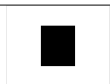	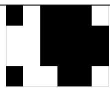		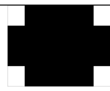	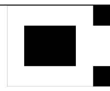
No. of patches	2	3	4	15	8	20	8
η_1 [%]	3.00	8.31	20.31	46.08	59.41	92.74	32.06
f_1 [Hz]	208.33	210.67	224.70	255.58	221.74	189.26	235.57

Table 1: Example of obtained non-dominated solutions for piezoelectric patch distributions with equipotential conditions (top) and without (bottom)

The financial support of FCT, Fundação para a Ciência e Tecnologia, Portugal, through IDMEC, under LAETA, project UID/EMS/50022/2013 and inter-institutional project *Advanced materials for noise reduction: modeling, optimization and experimental validation*, is acknowledged.

References

[1] Erasmo Carrera, Salvatore Brischetto and Pietro Nali. Plates and Shells for Smart Structures: Classical and Advanced Theories for Modeling and Analysis. John Wiley & Sons, Chichester, United Kingdom, 2011.

[2] A. L. Araújo, J. F. A. Madeira, C. M. Mota Soares and C. A. Mota Soares. Optimal Design for Active Damping in Sandwich Structures Using the Direct MultiSearch Method. Composite Structures, 105:29-34, 2013.

Active vibration control for a FGPM smart structure

Jonas Maruani, Isabelle Bruant, Frederic Pablo, Laurent Gallimard

Abstract Conventional smart structures suffer high stresses concentration near interlayer surfaces because of abrupt changes in electro-mechanical properties [1]. Moreover, the bounding agent may crack at low temperature and creep or pell at high temperature. These drawbacks can lead to severe deteriorations in both interlayer bounding strength and response performance. The FGPM, a new class of the well known functionally graded material (FGM), have attracted much attention these last years. They are designed to achieve a functional performance with gradually variable mechanical and piezoelectric properties in one or several directions. This continuity allows to avoid the aforementioned disadvantages of classical piezoelectric smart structures [2,3]. In this paper, static and dynamic behaviour of a thin structure made of functionally graded piezoelectric material (FGPM) is studied. The material properties of the PZT4/aluminium FGPM are graded in the thickness direction according to a fraction volume power law distribution. Top and bottom external surfaces are made of pure PZT4 and the mid plate of pure aluminium. The percolation phenomenon is taken into account. In static simulations both actuator and sensor efficiencies are studied. In dynamic simulations active vibration control is performed using a LQR method with an observer.

1 Results

The material properties of PZT4/Aluminium FGPM follow a fraction volume power law of distribution (govern by the fraction index k). The percolation phenomena occurs when there are enough metallic particles to form a conductive path into the mixture (i.e. when the percolation threshold V_c is reached). It induces a slicing in two electrical behaviour, insulating and conductive (Figures 1 and 2).

Laboratoire Energétique, Mécanique, Électromagnétisme, EA 4416, Université Paris Nanterre, 50 rue de Sèvres 92410 Ville d'Avray, France, e-mail: jonas.maruani@u-paris10.fr

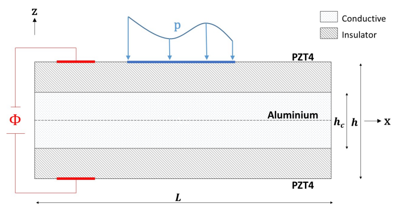

Fig. 1 FGPM beam model

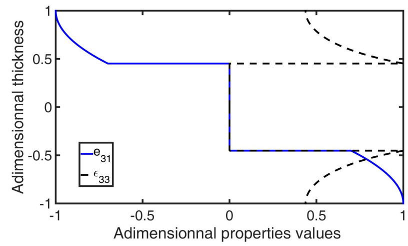

Fig. 2 Effective properties through the thickness for $k = 2$ and $V_c = 0.3$

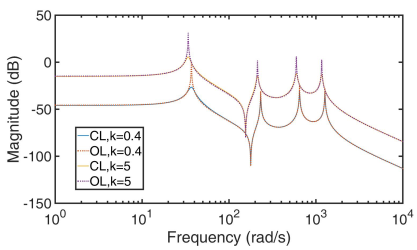

Fig. 3 Bode diagram for $k = 0.4$ and $k = 5$ with $V_c = 0.3$

Figure 3 presents bode diagrams of a cantilever beam for two values of k, in open loop (OL) and in closed loop (OP). The first four peaks are attenuated and show the efficiency of active vibration control.

2 Conclusion

The simulations results show that this FGPM smart structure is efficient in shape control and active vibration control. Parametric studies on the index k and on the percolation threshold V_c have been performed. The fraction index k has a huge influence on FGPM's sensing and actuation capabilities, the percolation threshold V_c has a minor role in them. Different values of k are optimal according to the uses, the sensing capability is optimised for high value of both k and V_c and low values of this both parameters optimise the actuation. This FGPM smart structure can perform active vibration control for a large range of values for k and shows its best performance when its actuation capability is optimised.

References

1. Preumont, André & al: Vibration control of active structures: an introduction. pringer Science & Business Media **179**, 143–152 (2011)
2. Komijani, M. & al: Vibration of thermo-electrically post-buckled rectangular functionally graded piezoelectric beams. Composite Structures **98**, 143–152 (2013)
3. Sharma & al: Finite element analysis on active vibration control using lead zirconate titanate–Pt–based functionally graded piezoelectric material. Journal of Intelligent Material Systems and Structures **27**, 490-499 (2016)

Effect of magnetic field on free and forced vibrations of laminated cylindrical shells containing magnetorheological elastomers

G. Mikhasev[1*], E. Korobko[2], S. Maevskaya[3], I. Mlechka[4]

[1,4] Belarusian State University, Nezavisimosti Ave., 4, Minsk 220030, Belarus

[2]A. V. Lykov Heat and Mass Transfer Institute of National Academy of Sciences of Belarus, P. Brovki Str., 15, Minsk 22072, Belarus

[3]Vitebsk State University, Moskovsky Ave., 33, Vitebsk, 210036, Belarus

Abstract

Free and forced vibrations of thin medium-length laminated cylindrical shells and panels assembled from elastic materials and magnetorheological elastomer (MRE) embedded between elastic layers are studied. Equivalent single layer model based on the generalized kinematic hypotheses of Timoshenko is used for the dynamic simulation of laminated shells. The high emphasis is placed on forced resonance vibrations and their suppressions by means of applied magnetic field.

1 Setting the problem

We consider a thin medium-length laminated cylindrical shell consisting of N transversely isotropic layers. The shell may be not circular and its edges are not necessarily plane curves. For elastic layers, the Young's and shear moduli E_k, G_k are constant real parameters, and for viscoelastic laminas made of the MRE, they are complex functions of the magnetic field induction B. For the MRE, the dependence of G_k is specified in [1]. The shell is under action of a normal periodic force $q_n(x,\varphi)\cos\omega_e t$, where x,φ are axial and circumferential coordinates, respectively, t is time, and ω_e is an excitation frequency. At the edges $x = x_1(\varphi), x = x_2(\varphi)$, the two groups of boundary conditions, the clamped support and simple support groups, are considered. Equivalent single layer model by Grigolyuk and Kulikov [2] based on the generalized kinematic hypotheses of Timoshenko is used in our study. If vibrations occur with formation of a large number of waves although in one direction at the shell surface, this model is represented by the system of three differential equations with respect to the displacement, stress and shear functions, χ, Φ, ϕ, respectively, with coefficients being functions of the reduced complex Young's and shear moduli, E, G. As long as E, G are expressed in terms of the complex shear modulus G_k for the MRE-layers, coefficients of the governing equations depend on the induction B of a magnetic field [2]. Thus, changing the intensity of a magnetic field, one can affect the dynamic characteristics of the shell (natural frequencies and modes) and control forced vibrations eliminating the resonance effects. The basic goal of our paper is to study the influence of an applied magnetic field on both free and forced vibrations. In the case of forced vibrations, the high emphasis is placed on the suppression of resonance vibrations.

*Corresponding author: G. I. Mikhasev, e-mail: mikhasev@bsu.by

2 Free vibrations

For a start, we consider free vibrations ($q_n \equiv 0$) of a circular shell or panel with plane edges ($x = x_1, x_2$ are constants). When the edges are simply supported with diaphragms preventing shears in their plane, then the required functions χ, Φ, ϕ are found in the explicit form. If one of the edges is free from a diaphragm, the boundary-value problem is solved by using the asymptotic approach, a solution being constructed in the form of the superposition of functions describing the main stress-state and the edge effect integrals. Then we consider a non-circular laminated cylinder or panel with oblique edges satisfying different variants of boundary conditions. By using the asymptotic approach [3], the natural modes are constructed in the form of functions localized near some generatrix called the weakest one.

We show that for medium-length MRE-sandwich shells and panels, the lowest natural frequencies and corresponding eigen-modes turn out to be more sensitive to the applied magnetic field.

2 Resonance vibrations and their suppression

In the case of forced vibrations, the amplitude $q_n(x,\varphi)$ of the external force, initial displacements and velocities, and all required functions χ, Φ, ϕ as well are expended into series in the natural modes of the shell. At first, we study the forced vibrations at some initial interval of time $t \in [0, t_B]$ at which a magnetic field is absence. Then solutions found at $t = t_B$ are assumed as the initial conditions for the initial boundary-value problem considered for $t \in [t_B, \infty)$ and $B \neq 0$. Since the adaptive MRE-shell gains new viscoelastic properties at $t = t_B$, the initial conditions, the amplitude $q_n(x,\varphi)$ and all required functions should be expended again into series in new natural modes “acquired” by the shell at $t = t_B$. It should be noted that high-frequency response of the shell to the impact application of the magnetic field is not taking here into account. We have performed the analysis of the amplitude-frequency characteristic for some distributions of the external force $q_n(x,\varphi)$ at different levels of the applied magnetic field and studied the damping capability of the utilized MRE [1]. We have revealed that applying magnetic field results in shifting the natural frequencies spectrum and guaranties a quick suppression of the resonance vibrations with frequencies ω_e being close to one of the lowest natural frequencies of the laminated MRE shell or panel.

References

[1] G.I. Mikhasev, H. Altenbach, E.A. Korchevskaya, On the influence of the magnetic field on the eigenmodes of thin laminated cylindrical shells containing magnetorheological elastomer, Composite Structures , 2014, vol. 113, pp. 186-196.

[2] E.I. Grigolyuk, G.M. Kulikov, Multilayer Reinforced Shells: Calculation of Pneumatic Tires, Moscow: Mashinostroenie, 1988 [in Russian]

[3] G.I. Mikhasev, P.E. Tovstik, Localized Vibrations and Waves in Thin Shells. Asymptotic Methods. Moscow: FIZMATLIT, 2009 [in Russian].

Flexure and buckling actuation in bilayer gel beams

Paola Nardinocchi and Eric Puntel

Abstract Soft active materials admit deformations and displacements that can be triggered through a wide range of external stimuli. We focus on a bilayer beam under chemical stimulus as a prototypical example of actuator which can both bend and buckle under swelling. Our simplified approach aims at obtaining simple design oriented formulas. Steady configurations are considered and the slow solvent diffusion is uncoupled by the fast elastic response of the material. We discuss a few interesting results based on a beam model approximation of the problem: snap buckling of shallow bilayer gel arches and surface wrinkling of the beam when the top layer is much softer and thinner than the bottom.

1 The beam model

This model was developed in [1] and further investigated in [2, 3]. The beam we are studying is realized bonding a hydrogel layer with Young modulus Y_b on the bottom of another layer with Young modulus $Y_t = \alpha Y_b$ ($\alpha < 1$); λ_{ob} and λ_{ot} are the corresponding free–swelling ratios which the two layer would have if swollen under free conditions. We denote by $h_t = \beta h$ and $h_b = h - h_t$ the thicknesses of the top and bottom layers, respectively, being h the thickness of the beam. When immersed into a solvent bath, due to the mismatch between the two layers, the beam bends. We assume that the visible bent deformation of the beam can be described by only considering longitudinal strains and stresses, and their pattern along the beam thickness. Hence, we introduce the visible longitudinal deformation λ of the beam as

Paola Nardinocchi
Sapienza Università di Roma, Rome (Italy), e-mail: paola.nardinocchi@uniroma1.it

Eric Puntel
Università di Udine, Udine (Italy) e-mail: eric.puntel@uniud.it

$$\lambda(x_3) = \Lambda_0(1 + x_3\Lambda_0\kappa)\,, \tag{1}$$

in terms of the uniform, possibly large, longitudinal stretch Λ_0 and the uniform curvature κ of the beam axis ($\kappa > 0$), $-h/2 \leq x_3 \leq h/2$ being the thickness coordinate in the dry configuration. Longitudinal stresses arise, due to the elastic deformations $\lambda_{et} = \lambda\lambda_{ot}^{-1}$ and $\lambda_{eb} = \lambda\lambda_{ob}^{-1}$ which recover the structural integrity of the beam. Imposing that the resultant axial force and bending moment are zero on each cross section, closed form formulas for Λ_0 and κ are obtained as a function of parameters α, β and Γ.

2 Results

Our first results show that: (**i**) as expected, beam curvature is zero in homogeneous beams, that is, for $\beta = 0, 1$ (see panel (a)); (**ii**) simplified model and accurate computation based on a fully 3D nonlinear stress–diffusion model excellently agree (see dotted and solid lines, respectively, in panel (a); (**iii**) a non monotonic response in terms of curvature is obtained, which apparently, is contrary to Timoshenko's predictions [4].

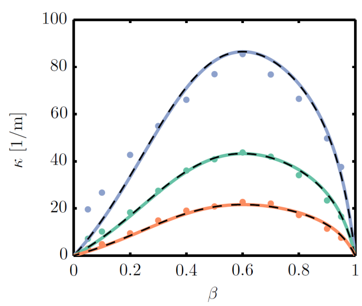

(a) Curvature κ vs. β for $\alpha = 0.3$, $Y_t = 45$kPa and height/width $= 1, 2, 4$: model vs. FEM analyses. [1]

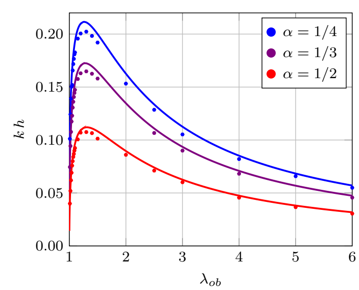

(b) Curvature times thickness κh versus freeswelling stretch λ_{ob} of the bottom layer for $\beta = 1/2$: model vs FEM analyses (dots) [3]

References

[1] Lucantonio A, Nardinocchi P, Pezzulla M (2014) Swelling-induced and controlled curving in layered gel beams 470(2171), DOI 10.1098/rspa.2014.0467
[2] Nardinocchi P, Puntel E (2016) Finite bending solutions for layered gel beams. International Journal of Solids and Structures 90:228–235
[3] Nardinocchi P, Puntel E (2017) Unexpected hardening effects in bilayered gel beams. Meccanica (in press)
[4] Timoshenko S (1925) Analysis of bimetal thermostats. JOSA 11:233–255

Finite element analysis of effective properties of ceramic piezocomposites by using different homogenization approaches

A.V. Nasedkin*, A.B. Kudimova

Southern Federal University, Miltchakova str., 8a, Rostov on Don 344090, Russia

Abstract

The paper presents an investigation of effective properties of piezocomposites of type microporous piezoceramic/polycrystallites type with the help of represented using the effective moduli method, the computer modeling of representative volumes with random structure of heterogeneity and the finite element method to solve the homogenization problems. The effective moduli, obtained from the problems with different boundary conditions on the edges of representative volumes, are analyzed.

1 Objectives

Piezoelectric materials are widely used in modern engineering because due to the piezoelectric effect they enable to convert electrical energy into mechanical energy and vice versa. In order to improve the efficiency of these materials, the piezoelectric composites based on piezoceramic matrices has been developed recently. Porous piezoceramic materials appeared perspective for use as the elements for acoustic transmitters and as renewable energy sources. As it turned out, in comparison with dense ceramics, porous piezoceramics had small acoustic impedance, but sufficiently high values of piezoelectric sensitivities and thickness piezomoduli. However, porous piezoceramics is less strong compared with dense ceramics. To improve the mechanical properties of porous piezoceramics, more rigid crystallites can be added into ceramic composites.
The subject of this research is the piezocomposites of porous piezoceramics/crystallite type. Photomicrographs of these piezocomposites, obtained in the Research Institute of Physics, Southern Federal University [3], are shown in Fig. 1. From these figures it can be seen that the pores in piezoceramics are ten times smaller than the sizes of crystallites. Therefore, for such complex three-phase material the homogenization can be carried out in two stages. At the first stage, the effective moduli of porous piezoceramics can be calculated, and at the second stage the effective moduli of two-phase composite ceramic/crystallites can be determined.

*A. V. Nasedkin, e-mail: nasedkin@math.sfedu.ru

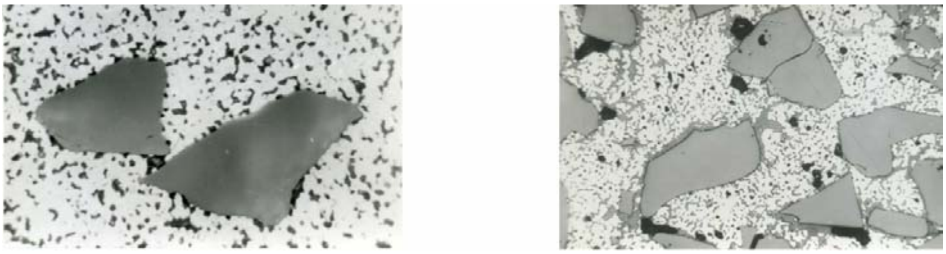

Figure 1. Micrographs of ceramic composites with different percentage of inclusion

2 Homogeneous techniques and results

We develop the effective moduli method and finite element technique in accordance with [1, 2]. To find the effective moduli of an inhomogeneous body, we set four static piezoelectric problems for a representative volume. These problems differ by the boundary conditions which are set on the representative volume surfaces. Special formulas are derived to calculate the effective moduli of piezoelectric media with arbitrary anisotropy. Based on these formulas, we find the full set of effective moduli for ceramic polycrystalline piezocomposites using finite element method. As a representative volume, we consider a cube evenly divided into cubic piezoelectric finite elements. At the first stage, depending on the given porosity the material properties of range of randomly selected finite elements are modified to the properties of pores. Further from the solutions of homogenization problems we determine the effective moduli of the porous piezoceramics. At the second stage, the same procedures are used for the composite made of piezoceramics and crystallites. To provide an example, we consider polycrystalline piezoceramics with sapphire (α-corundum) crystallites Al_2O_3 as inclusions. The effective moduli for inclusions are calculated as the average moduli of monophase polycrystallite of trigonal system. The results of calculations give the full set of effective moduli.

Acknowledgements. The work was supported by the Ministry of Education and Science of Russia, competitive part of state assignment, No. 9.1001.2017/PCh.

References

[1] S.V. Bobrov, A.V. Nasedkin, A.N. Rybjanets, Finite element modelling of effective moduli of porous and polycrystalline composite piezoceramics, in: Proc. VIII Int. Conf. on Computational Structures Technology, B.H.V. Topping, G. Montero, R. Montenegro, (Eds), Civil-Comp Press, Stirlingshire, UK, Paper 107, 2006.

[2] A.V. Nasedkin, M.S. Shevtsova, Improved finite element approaches for modeling of porous piezocomposite materials with different connectivity, in: Ferroelectrics and Superconductors: Properties and Applications, Ed. I.A. Parinov, Nova Science Publishers, New York, 2011, pp. 231–254.

[3] A.N. Rybyanets, A.A. Rybyanets, Ceramic piezocomposites: Modeling, technology, and characterization, IEEE Transactions on Ultrasonics, Ferroelectrics, and Frequency Control, 2011, vol. 58(9), pp. 1757–1773.

Hybrid-mixed finite element method for piezoelectric shells through a sampling surfaces formulation

S. V. Plotnikova[1*], G. M. Kulikov[1], E. Carrera[2]

[1] Laboratory of Intelligent Materials and Structures
Tambov State Technical University, Sovetskaya, 106, Tambov 392000, Russia
[2] Department of Mechanical and Aerospace Engineering
Politecnico di Torino, Corso Duca degli Abruzzi, 24, 10129 Turin, Italy

Abstract

A hybrid-mixed exact geometry four-node piezoelectric solid-shell element using the sampling surfaces (SaS) technique is developed. The SaS formulation is based on choosing inside the nth layer I_n SaS located at Chebyshev polynomial nodes in order to introduce the displacements and electric potentials of these surfaces as basic shell variables. Such choice of unknowns with the consequent use of Lagrange polynomials of degree $I_n - 1$ in the thickness direction for displacements, strains, electric potential and electric field allows the presentation of the laminated piezoelectric shell formulation in a very compact form. The proposed hybrid-mixed four-node piezoelectric solid-shell element is based on the Hu-Washizu variational equation and exhibits a superior performance in the case of coarse meshes. It could be useful for the 3D stress analysis of thick and thin doubly-curved laminated piezoelectric shells since the SaS formulation gives the possibility to obtain numerical solutions with a prescribed accuracy, which asymptotically approach the exact solutions of electroelasticity as the number of SaS tends to infinity.

1 Hu-Washizu Variational SaS formulation

Consider a laminated shell of the thickness *h*. Let the middle surface Ω be described by orthogonal curvilinear coordinates θ_1 and θ_2, which are referred to the lines of principal curvatures of its surface. The coordinate θ_3 is oriented along the unit vector normal to the middle surface. According to the SaS concept, we choose inside the *n*th layer I_n SaS $\Omega^{(n)1}, \Omega^{(n)2}, ..., \Omega^{(n)I_n}$ located at Chebyshev polynomial nodes and interfaces $\Omega^{[n-1]}$ and $\Omega^{[n]}$ as well, where the index $n = 1,2,...,N$ identifies the belonging of any quantity to the *n*th layer; *N* is the number of layers.

The through- thickness SaS approximations [1] can be written as

$$[u_i^{(n)}\ \varepsilon_{ij}^{(n)}\ \sigma_{ij}^{(n)}\ \varphi^{(n)}\ E_i^{(n)}] = \sum_{i_n} L^{(n)i_n} [u_i^{(n)i_n}\ \varepsilon_{ij}^{(n)i_n}\ \sigma_{ij}^{(n)i_n}\ \varphi^{(n)i_n}\ E_i^{(n)i_n}], \tag{1}$$

where $u_i^{(n)}, \varepsilon_{ij}^{(n)}, \sigma_{ij}^{(n)}, \varphi^{(n)}, E_i^{(n)}$ are the displacements, strains, stresses, electric potential and electric field of the *n*th layer; $u_i^{(n)i_n}, \varepsilon_{ij}^{(n)i_n}, \sigma_{ij}^{(n)i_n}, \varphi^{(n)i_n}, E_i^{(n)i_n}$ are the displacements,

*Corresponding author: S.V. Plotnikova, e-mail: plotnikovasvetlana62@gmail.com

strains, stresses, electric potential and electric field of SaS of the nth layer $\Omega^{(n)i_n}$; $L^{(n)i_n}(\theta_3)$ are the Lagrange basis polynomials of degree $I_n - 1$ corresponding to the nth layer:

$$L^{(n)i_n} = \prod_{j_n \neq i_n} \frac{\theta_3 - \theta_3^{(n)j_n}}{\theta_3^{(n)i_n} - \theta_3^{(n)j_n}} \quad (i_n, j_n = 1, 2, ..., I_n), \tag{2}$$

where the indices i_n, j_n identify the belonging of any quantity to the SaS of the nth layer.

The proposed hybrid-mixed piezoelectric solid-shell element is based on the Hu-Washizu variational equation of electroelasticity in which displacements, strains and stresses are utilized as independent variables [2]:

$$\delta \iint_{\Omega} \sum_n \int_{\theta_3^{[n-1]}}^{\theta_3^{[n]}} \left[\frac{1}{2} \eta_{ij}^{(n)} C_{ijkl}^{(n)} \eta_{kl}^{(n)} - E_k^{(n)} e_{kij}^{(n)} \eta_{ij}^{(n)} - \frac{1}{2} E_i^{(n)} \in_{ij}^{(n)} E_j^{(n)} - \sigma_{ij}^{(n)} (\eta_{ij}^{(n)} - \varepsilon_{ij}^{(n)}) \right] dV = \delta W, \tag{3}$$

where $dV = A_1 A_2 (1 + k_1 \theta_3)(1 + k_2 \theta_3) d\theta_1 d\theta_2 d\theta_3$ is the infinitesimal volume element; A_1, A_2 and k_1, k_2 are the coefficients of the first fundamental form and principal curvatures of the middle surface; $\theta_3^{[n-1]}$ and $\theta_3^{[n]}$ are the transverse coordinates of interfaces; $\varepsilon_{ij}^{(n)}$ and $\eta_{ij}^{(n)}$ are the displacement-dependent and displacement-independent strains; $C_{ijkl}^{(n)}$, $e_{kij}^{(n)}$ and $\in_{ij}^{(n)}$ are the elastic, piezoelectric and dielectric constants; W is the work done by external electromechanical loads. Here, the summation on repeated Latin indices is implied.

Following the SaS technique (1), we introduce the next assumption of the hybrid-mixed solid-shell element formulation. Assume that the displacement-independent strains are distributed through the thickness of the nth layer as follows:

$$\eta_{ij}^{(n)} = \sum_{i_n} L^{(n)i_n} \eta_{ij}^{(n)i_n}, \tag{4}$$

where $\eta_{ij}^{(n)i_n}$ are the displacement-independent strains of SaS of the nth layer.

2 Finite element formulation

The finite element formulation is based on a simple interpolation of the shell via exact geometry four-node piezoelectric solid-shell elements

$$u_i^{(n)i_n} = \sum_r N_r u_{ir}^{(n)i_n}, \quad \varphi^{(n)i_n} = \sum_r N_r \varphi_r^{(n)i_n}, \tag{5}$$

where $N_r(\xi_1, \xi_2)$ are the bilinear shape functions of the element; $u_{ir}^{(n)i_n}$ and $\varphi_r^{(n)i_n}$ are the displacements and electric potentials of SaS $\Omega^{(n)i_n}$ at element nodes; ξ_1, ξ_2 are the normalized curvilinear coordinates θ_1, θ_2; the nodal index r runs from 1 to 4. The term "exact geometry" reflects the fact that the parametrization of the middle surface is known a priori and, therefore, the coefficients of the first and second fundamental forms are taken exactly at element nodes.

To implement the efficient analytical integration throughout the element, the enhanced ANS method is employed:

$$\varepsilon_{ij}^{(n)i_n} = \sum_r N_r \varepsilon_{ijr}^{(n)i_n}, \quad E_i^{(n)i_n} = \sum_r N_r E_{ir}^{(n)i_n}, \tag{6}$$

where $\varepsilon_{ijr}^{(n)i_n}$ and $E_{ir}^{(n)i_n}$ are the displacement-dependent strains and electric field of SaS of the nth layer at element nodes. The main idea of such approach can be traced back to the ANS method developed by many scientists for the isoparametric finite element formulation. In contrast with above formulation, we treat the term "ANS" in a broader sense. In the proposed exact geometry four-node solid-shell element formulation, all components of the displacement-dependent strain tensor and electric field vector are assumed to vary bilinearly throughout the biunit square in (ξ_1, ξ_2)-space.

To overcome shear and membrane locking and have no spurious zero energy modes, the robust stress and displacement-independent strain interpolations [3] are utilized:

$$\left[\sigma_{11}^{(n)i_n}\ \sigma_{22}^{(n)i_n}\ \sigma_{33}^{(n)i_n}\ \sigma_{12}^{(n)i_n}\ \sigma_{13}^{(n)i_n}\ \sigma_{23}^{(n)i_n}\right]^{\mathrm{T}} = \mathbf{P}\boldsymbol{\Phi}^{(n)i_n}, \quad \boldsymbol{\Phi}^{(n)i_n} = \left[\Phi_1^{(n)i_n}\ \Phi_2^{(n)i_n}\ \ldots\ \Phi_{12}^{(n)i_n}\right]^{\mathrm{T}}, \tag{7}$$

$$\left[\eta_{11}^{(n)i_n}\ \eta_{22}^{(n)i_n}\ \eta_{33}^{(n)i_n}\ \eta_{12}^{(n)i_n}\ \eta_{13}^{(n)i_n}\ \eta_{23}^{(n)i_n}\right]^{\mathrm{T}} = \mathbf{P}\boldsymbol{\Psi}^{(n)i_n}, \quad \boldsymbol{\Psi}^{(n)i_n} = \left[\Psi_1^{(n)i_n}\ \Psi_2^{(n)i_n}\ \ldots\ \Psi_{12}^{(n)i_n}\right]^{\mathrm{T}}, \tag{8}$$

$$\mathbf{P} = \begin{bmatrix} 1 & 0 & 0 & 0 & 0 & 0 & \xi_2 & 0 & 0 & 0 & 0 & 0 \\ 0 & 1 & 0 & 0 & 0 & 0 & 0 & \xi_1 & 0 & 0 & 0 & 0 \\ 0 & 0 & 1 & 0 & 0 & 0 & 0 & 0 & \xi_1 & \xi_2 & 0 & 0 \\ 0 & 0 & 0 & 1 & 0 & 0 & 0 & 0 & 0 & 0 & 0 & 0 \\ 0 & 0 & 0 & 0 & 1 & 0 & 0 & 0 & 0 & 0 & \xi_2 & 0 \\ 0 & 0 & 0 & 0 & 0 & 1 & 0 & 0 & 0 & 0 & 0 & \xi_1 \end{bmatrix}$$

that provides a correct rank of the element stiffness matrix.

Substituting first the through-thickness SaS approximations (1), (4) and then the finite element interpolations (5)-(8) into the Hu-Washizu variational equation (3), we arrive at the element equilibrium equations. After the elimination of column matrices $\boldsymbol{\Phi}^{(n)i_n}$ and $\boldsymbol{\Psi}^{(n)i_n}$ on the element level, the following system of linear equations are obtained:

$$\mathbf{KU} = \mathbf{F},$$

where $\mathbf{K}$ is the element stiffness matrix of order $12N_{\mathrm{SaS}} \times 12N_{\mathrm{SaS}}$; $\mathbf{U}$ is the element displacement vector; $\mathbf{F}$ is the element-wise surface traction vector; $N_{\mathrm{SaS}} = \sum_n I_n - N + 1$ is the total number of SaS.

It is worth noting that the element stiffness matrix is evaluated without using the expensive numerical matrix inversion that is impossible in available isoparametric hybrid-mixed finite element formulations.

References

[1] G.M. Kulikov, S.V. Plotnikova, A sampling surfaces method and its application to three-dimensional exact solutions for piezoelectric laminated shells, Int. J. Solids Struct., 2013, vol. 50, pp. 1930–1943.

[2] G.M. Kulikov, S.V. Plotnikova, The use of 9-parameter shell theory for development of exact geometry 12-node quadrilateral piezoelectric laminated solid-shell elements, Mech. Advanced Mater. Struct., 2015, vol. 22, pp. 490–502.

[3] G.M. Kulikov, S.V. Plotnikova, Non-linear exact geometry 12-node solid-shell element with three translational degrees of freedom per node, Int. J. Numer. Methods Eng., 2011, vol. 88, pp. 1363–1389.

A case study of smart structure design using additive manufacturing to emulate a functionally graded material

A. M. R. Ribeiro*, M. Leite, A. Carvalho

IDMEC – IST, Universidade de Lisboa, Portugal

Abstract

Functionally Graded Materials can be considered a class within the so called Smart Materials; its main concept suggests a continuous variation of properties along the geometry of single part (Miyamoto, 2013). At the present state of technology, practical implementation is often obtained stepwise, with relatively thin layers, so that although the variation is not strictly continuous, the change is small enough to avoid problems due to interfaces with very different properties. This approach suits nicely in the Additive Manufacture family of manufacturing processes that also build thin layers, one upon the other (Gibson, 2010). The present work builds on these remarks but addresses the problem of grading properties, not by changing the bulk properties but by changes in the internal structure of the part across its domain.

The utilization of Smart Structures in general or Functionally Graded Materials in particular is considered typically case dependent, at least in the present state of the art. So, this work intends to show how to address a particular problem from the above standpoint.

Airfoil design implies addressing a number of concurrent issues, such as aerodynamics, structures and materials. Among the several specifications that must be met, is the need to control pitch (the angle between the line of neutral lift and the apparent direction of the wind) along the airfoil's length. This problem is now actively addressed in helicopters' design. In this case, a Smart Material that intrinsically controls the pitch along the airfoil length – a Smart Airfoil – would be most welcome. The present work aims at contributing to the design of Smart Airfoils.

Another conspicuous problem with airfoils is their dynamic behavior. Vibrations in airfoils are quite undesirable, not only because they can lead to material fatigue but also because they interact with the flow. One of the main problems is flutter, a situation where structural resonances in the airfoil couple with flow oscillations of the surrounding fluid, eventually resulting in instable flight and increasing deformations of the airfoil that can lead to it being ripped out (Srinivasan, 1997). Vibration control is needed. Both active control and passive damping are used to avoid or, at least, delay flutter situations. Material damping due to hysteresis is usually not enough and this work also contemplates the use of the internal structure to obtain increased attenuation of large amplitude vibrations as o tool to delay the destructing effects of flutter.

According to the above, a test part will be designed, built and studied. This part shall have a geometry suited to assess qualitatively the possibility of using the internal structure to

* Corresponding author: A.M.R. Ribiero, e-mail: relogio.ribeiro@tecnico.ulisboa.pt

inherently change pitch accordingly to aerodynamic loads and avoid deformations large enough to be dangerous to its structural integrity.
During the design phase, numerical simulations will be performed using Finite Element Method commercial software. This simulations will be used only as guiding hints for the design, not as a reliably precise prediction of the specimen behavior due to the difference usually existing between the nominal (bulk) mechanical properties of the materials and the effective (experimental) properties exhibited in Additive Manufacture printed parts.
The chosen geometry will be built in a Fusion Deposition Material 3D printer from MarkForged® using a polyamide. Both quasi-static and dynamic tests will be performed on this specimen. The quasi-static tests will be used to study the possibility of using this kind of approach to build Smart Airfoils. The vibration tests will be made using Experimental Modal Analysis techniques in order to study amplitude related nonlinearities capable of delaying flutter.

References

[1] Y. Miyamoto, et al., eds., Functionally Graded Materials: Design, Processing and Applications, Springer Science & Business Media, 2013, Vol. 5.

[2] I. Gibson, D. Rosen, B. Stucker, Additive Manufacturing Technologies, New York: Springer, 2010, Vol. 238.

[3] A.V. Srinivasan, Flutter and resonant vibration characteristics of engine blades: An igti scholar paper, ASME 1997 International Gas Turbine and Aeroengine Congress and Exhibition, American Society of Mechanical Engineers, 1997.

Numerical investigation on polarization effects within electrochemical cells

M. Rossi[1], **T. Wallmersperger**

Institut für Festkörpermechanik, TU Dresden
George-Bähr-Str. 3c, D-01069 Dresden, Germany

Abstract

Energy storage and release in the field of electrochemical devices is an attractive topic for the scientific community. Electrochemical cells (ECs) are expected to play a significant role in the next generation energy systems for use in vehicles as a replacement to combustion engines (minimum environmental impact due to carbon dioxide reduced emissions) [1]. These ECs can transform chemical into electrical energy (galvanic cells) and vice versa (electrolytic cells).
In the present research, an electrochemical model is applied for a thin film sandwiched between flat porous electrodes under input voltage conditions. A parametric analysis is carried out in order to evaluate the influence on the model of the main material parameters. Furthermore, polarization effects are investigated. In fact, in literature (e.g. [2, 3]) it is shown that polarization effects at the electrode/electrolyte interface are fundamentals for microelectrochemical systems; these employ thin films such as micro-batteries and proton-exchange-membrane fuel cells. In the present work, time-dependent numerical simulations within a finite element method framework are performed.

1 Electrochemical model

A continuum-based model is developed in order to describe the behavior of Nafion membranes (electrolytic thin films) sandwiched between flat porous electrodes (mostly made of graphite). Within the electrolytic membrane, cations (produced and consumed at the reaction planes through chemical reactions) are free to move, while anions (counterions) are fixed. Configurations like these are suitable for a wide range of electrochemical applications: fuel cells, chlor-alkali and water electrolysers and in surface-treated metals. As shown in Fig. 1, part of the membrane (named polarization or Stern layer) and the electrodes are outside the computational domain. In fact, due to polarization effects, ions form a stacked structure at the electrode/electrolyte interface. Therefore, the planes where chemical reactions occur (named reaction planes) shift from the electrode/electrolyte interface towards the inside of the field.
The fully-coupled electrochemical model is based on the Poisson-Nernst-Planck (PNP) theory: diffusive-migrative charge transport and electric field distribution are described by a system of nonlinear partial differential equations [4].
Boundary conditions involve polarization effects, described by the Stern Layer (SL) theory, and electrochemical kinetics, described by the Frumkin-Butler-Volmer (FBV) theory [2, 3]. The electrochemical model is set for potentiostatic conditions, therefore for an input applied voltage, such as for electrolytic cells.

[1]Corresponding Author: Marco Rossi, Phone: +49 351 463-39659, Fax: +49 351 463-32450, E-mail: marco.rossi@tu-dresden.de

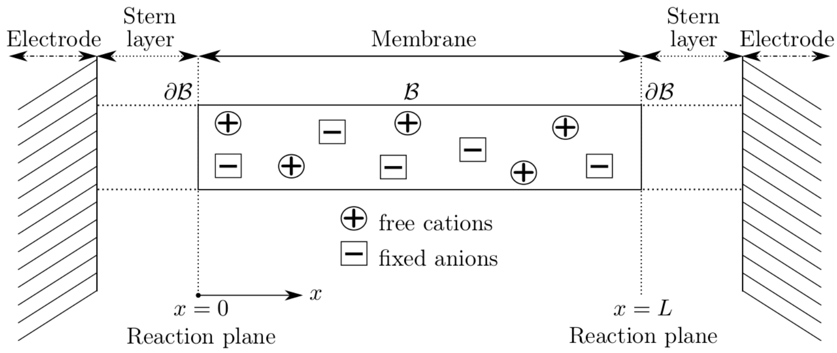

Figure 1: One-dimensional domain, $\mathcal{B} : 0 < x < L$ for the electrochemical cell model. The Stern layer has been depicted by increasing its original length.

2 Numerical Investigations

Finite element simulations for a one-dimensional domain are performed using the commercial tools: MATLAB and COMSOL Multiphysics. High gradients in the electrochemical boundary layers suggest to use a refined mesh as, for example, a logarithmic distribution along the x-direction [4].
According to the applied electrochemical model, two numerical investigations are carried out. First, a parametric analysis is performed in order to show the effect of different material parameters on the electrochemical variables: concentration $c(x,t)$ and electrical potential $\phi(x,t)$. Second, polarization effects are either included or excluded in the model.

3 Conclusion and Outlook

Polarization effects, as well as the main material parameters, can have a huge impact on the steady-state profile of the concentration and the electrical potential. The results show the influence of polarization effects with respect to standard models (e.g. [5]) where this phenomenon is neglected.
Many others phenomena can be modeled in order to extend the model proposed in this work. In further research, ohmic drop in the metal electrodes and the interactions with the mechanical field within the thin membrane will be investigated.

References

[1] C. Thomas, Fuel cell and battery electric vehicles compared, International Journal of Hydrogen Energy, vol. 34, no. 15, pp. 6005-6020, 2009

[2] M. Z. Bazant, K. T. Chu, and B. J. Bayly, Current-voltage relations for electrochemical thin films, SIAM Journal on Applied Mathematics, vol. 65, no. 5, pp. 1463-1484, 2005

[3] P. Biesheuvel, M. Van Soestbergen, and M. Bazant, Imposed currents in galvanic cells, Electrochimica Acta, vol. 54, no. 21, pp. 4857-4871, 200

[4] T. Wallmersperger, D. J. Leo, and C. S. Kothera, Transport modeling in ionomeric polymer transducers and its relationship to electromechanical coupling, Journal of Applied Physics, vol. 101, no. 2, pp. 024912, 2007

[5] A. V. Sokirko and F. H. Bark, Diffusion-migration transport in a system with butler-volmer kinetics, an exact solution, Electrochimica Acta, vol. 40, no. 12, pp. 1983-1996, 1995.

Influence of impactor's mass on internal resonances in nonlinear elastic doubly curved shells during impact interaction

Yu. A. Rossikhin, M. V. Shitikova, M. S. K. J. M. Saleh

Voronezh State Technical University, Research Center on Dynamics of Solids and Structures, 20-letiya Oktyabrya 84, Voronezh 394006, Russia

Abstract

Large amplitude (geometrically non-linear) vibrations of doubly curved shallow shells with rectangular base under the low velocity impact by an elastic sphere are investigated. The equations of motion are reduced to a set of infinite nonlinear ordinary differential equations of the second order in time and with cubic and quadratic nonlinearities in terms of the generalized displacements. Assuming that only two natural modes of vibrations dominate during the process of impact and applying the method of multiple time scales, the set of equations is obtained, which allows one to study internal resonances which could be initiated by the impact and to investigate the influence of impactor's mass on this process.

1 Introduction

Doubly curved panels are widely used in aeronautics, aerospace and civil engineering and are subjected to dynamic and impact loads that can cause vibration amplitude of the order of the shell thickness, giving rise to significant non-linear phenomena. In spite of the fact that the impact theory is substantially developed [1], there is a limited number of papers devoted to the problem of impact over geometrically nonlinear shells. The review in the field could be found in [2].

In the present paper, a new approach proposed recently for the analysis of the impact interactions of nonlinear doubly curved shallow shells with rectangular base under the low-velocity impact by an elastic sphere [2] is utilized for studying internal resonances which could be initiated during the impact.

2 Problem formulation and method of solution

Assume that an elastic or rigid sphere of mass M moves along the z-axis towards a simply supported thin walled doubly curved shell with thickness h, curvilinear lengths a and b, principle curvatures k_x and k_y and rectangular base. Impact occurs at the moment $t = 0$ with the velocity εV_0 (ε is a small value) at the point with Cartesian coordinates (x_0, y_0). According to Mushtari-Donnell's nonlinear shallow shell theory, the equations of motion could be obtained in terms of lateral deflection w and Airy's stress function ϕ [3]

$$\frac{1}{E}\left(\frac{\partial^4\phi}{\partial x^4}+2\frac{\partial^4\phi}{\partial x^2\partial y^2}+\frac{\partial^4\phi}{\partial y^4}\right)=-\frac{\partial^2 w}{\partial x^2}\frac{\partial^2 w}{\partial y^2}+\left(\frac{\partial^2 w}{\partial x\partial y}\right)^2-k_y\frac{\partial^2 w}{\partial x^2}-k_x\frac{\partial^2 w}{\partial y^2}, \qquad (1)$$

$$\frac{D}{h}\left(\frac{\partial^4 w}{\partial x^4}+2\frac{\partial^4 w}{\partial x^2\partial y^2}+\frac{\partial^4 w}{\partial y^4}\right)=\frac{\partial^2 w}{\partial x^2}\frac{\partial^2\phi}{\partial y^2}+\frac{\partial^2 w}{\partial y^2}\frac{\partial^2\phi}{\partial x^2}-2\frac{\partial^2 w}{\partial x\partial y}\frac{\partial^2\phi}{\partial x\partial y}+k_y\frac{\partial^2\phi}{\partial x^2}+k_x\frac{\partial^2\phi}{\partial y^2}+\varepsilon^k\frac{F}{h}-\rho\ddot{w},$$

where $D=\dfrac{Eh^3}{12(1-\nu^2)}$ is the cylindrical rigidity, ρ is the density, E and ν are the elastic modulus and Poisson's ratio, respectively, t is time, $F=P(t)\delta(x-x_0)\delta(y-y_0)$ is the contact force, $P(t)$ is yet unknown function, and δ is the Dirac delta function.
The equation of motion of the sphere and corresponding initial conditions are written as

$$M\ddot{z}=-P(t)\,,\qquad z(0)=0,\quad \dot{z}(0)=\varepsilon V_0, \tag{2}$$

where $z(t)$ is the displacement of the sphere, in so doing $z(t)=w(x_0,y_0,t)$.
Then suitable trial function that satisfies the geometric boundary conditions is represented in terms of the product of eigen functions and generalized time-dependent functions, and its substitution in equations (1) allows one to reduce the equations of motion to a set of infinite nonlinear ordinary differential equations of the second order in time and with cubic and quadratic nonlinearities in terms of the generalized displacements.
Since is it assumed that shell's displacements are finite, then the local bearing of the shell and impactor's materials could be neglected with respect to the shell deflection in the contact region. Assuming that only two natural modes of vibrations dominate during the process of impact and applying the method of multiple time scales, the set of dynamic equations is obtained, which allows one to find the time dependence of the contact force and to determine the contact duration and the maximal contact force.
It has been shown that the time dependence of the contact force depends essentially on the position of the point of impact and the parameters of two impact-induced modes coupled by the internal resonance. Besides, the contact force depends essentially on the magnitude of the initial energy of the impactor.

3 Conclusion

The proposed method allows one to reveal the possibilities for impact-induced internal resonances and to analyze the influence of impactor's parameters on the character of such internal resonances.

Acknowledgements

This research was supported by the Ministry of Education and Science of the Russian Federation (Project № 1.4907.2017/Leading Researcher).

References

[1] Yu. A. Rossikhin, M. V. Shitikova, A. Transient response of thin bodies subjected to impact: Wave approach, The Shock and Vibration Digest, 2007, vol. 39, pp. 273-309.

[2] Yu. A. Rossikhin, M. V. Shitikova, M. Salih Khalid, Dynamic response of a doubly curved shallow shell rectangular in plan impacted by a sphere, in: M. Ceraolo (Ed.), Proceedings of the 2014 International Conference on Mathematical Models and Methods in Applied Sciences, Vol. 32 of Mathematics and Computers in Science and Engineering Series, NAUN, 2014, pp. 109-113.

[3] Kh. M. Mushtari, K. Z. Galimov, Nonlinear Theory of Thin Elastic Shells (in Russian). Kazan', Tatknigoizdat, 1957 (English translation NASA-TT-F62, 1961).

Functional Interfaces and interphases in thermoplastic composites

D. Ruch*, A. Martin, G. Mertz, P. Dubois

Luxembourg Institute of Science and Technology (LIST), Materials Research Technology (MRT) department, 5 rue Bommel, L-4940 Hautcharage, Luxembourg.

Abstract

In this work, the challenging development of the fibre-matrix interfacial layer is addressed in the field of high performance thermoplastic composites reinforced with continuous carbon fibres. Particularly, an environmentally friendly methodology is used to modify carbon fibre surface in order to improve the compatibility and the quality of the fibre-matrix interface. Based on the supramolecular assembly of coatings obtained by adsorption and self-assembly of selected macromolecules onto solid surfaces, the study deals with the development of thin polymer films, namely sizing, having tailored structures and properties. This presentation will be focused (i) on the carbon fibre surface characterization and modification by water-based formulations applied in accordance with thermoplastic sizing treatments, (ii) on the discussion on the sizing intrinsic chemical network, (iii) on the interphase properties and (iv) on the mechanical performances of the resulted composites.

Finally, the contribution of this chemical approach will be discussed in the frame of developing the next generation of composites (actuators/sensors/morphing/MEMS, EMI shielding….).

* Corresponding author: D. Ruch, e-mail: david.ruch@list.lu

About magnetic field inside the structure of magnetized granulated material

A.A. Sandulyak[1*], A.V. Sandulyak[1], M.N. Polismakova[1], V.A. Ershova[1]

[1] Moscow technological university, Stromynka, 20, Moscow 107996, Russia

Abstract

By using of porous magnetic materials (for example, in magnetic separators, filters) the working element of which is magnetized granulated material with system of branched porous [1-4], one of the important task is to obtain the information about field parameters within porous, between grains, the intensity h in particular. The well-known models of granulated medium magnetization are usually reduced to the traditional determination of average magnetic permeability (susceptibility) and not permit to get an answer on the problem.

The idea of selective (some kind of channel-by-channel, or “shot”) magnetization is developed in papers [5-7] where elementary effective magnetic channels formed (in the rope form) along magnetization direction are responsible for magnetization of such a medium (fig.1). Self-organization of these channels is possible due to granules’ chains (mainly sinuous chains) that are always really manifested among a lot of skeletal granulated structure granules-chains chaotically located in the medium.

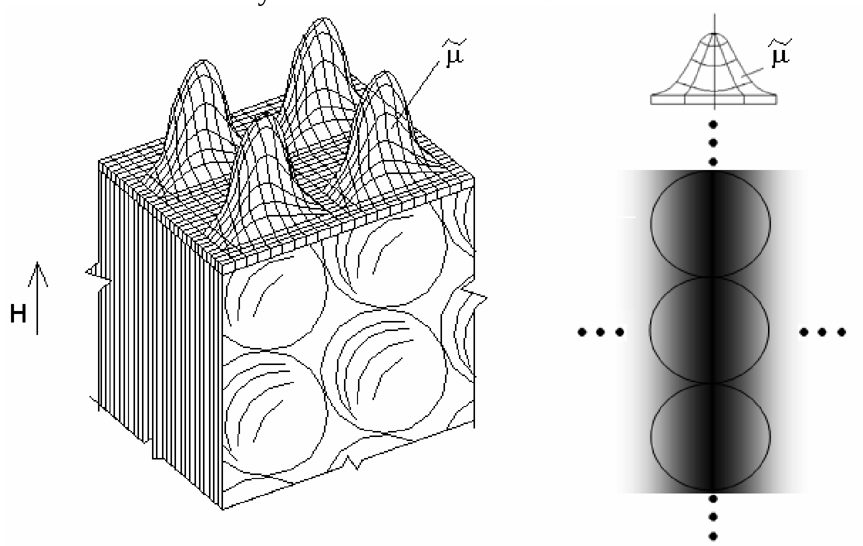

Figure 1: Illustration of selective (channel-by-channel) magnetization model of granulated medium with expressed shape (profile in section) of magnetic permeability $\tilde{\mu}$ for each effective (in the “rope”) magnetic channel [5]. One of them is shown separately: quasi-continuous longwise and condensing to axis line granules (balls) chain.

* Corresponding author: A. A. Sandulyak, e-mail: anna.sandulyak@mail.ru

Thereat each of these magnetic channels likened to quasi-continuous channel, although it may be characterized by average (by volume) permeability values [5-7], nevertheless, is not equivalent by cross section [5-7]. Thus, as far as the radius $r=r_c$ of its core and the radius $r=r_p$ of "growing" tubular layer increase, their magnetic resistance increases because of growing porous interlayer between R radius granules in the chain. It makes us considering new key characteristics such as "tube" permeability $\tilde{\mu}$ and core permeability $\langle\tilde{\mu}\rangle$ (certainly, the permeability of granules' material μ is known).

Conclusion

In this work according to the new model (different to traditional quasicontinuous model of determination of average magnetic permeability) are given peculiarities of "elementary" effective magnetic channel of granulated ferromagnetic material, i.e. channel in channel system, formed (in the rope form) along magnetization direction. Experimental and design data of magnetic permeability of quasicontinuous magnetic channel (for core $\langle\tilde{\mu}\rangle$ and tube $\tilde{\mu}$ with different radius) are determinate and compared. It was also determinate, that $\tilde{\mu}$ has extreme profile (by analogy with profile of liquid velocity in the tube) which is bell-shaped, in outward appearance similar to Gauss distribution. The possibility of using an expression for $\tilde{\mu}$ by calculation of field intensity $h=\tilde{\mu}H$ in either, one or another point on the defined distance from contact point of grains in the porous ferromagnetic material is confirmed.

Rererences

[1] X. Li, X.S. Li: Micro-macro quantification of the internal structure of granular materials, Journal of Engineering Mechanics, 2009, vol.135 (7), pp. 641–656.

[2] S. Arajs, C.A. Moyer, R. Aidun, E. Matijevic: Magnetic filtration of submicroscopic particles through a packed bed of spheres, Journal of Applied Physics, 1985, vol. 57, pp. 4286.

[3] J. Watson, S. Watson: The ball matrix magnetic separator, IEEE Transactions on Magnetics, 1983, vol.19, issue 6, pp. 2698–2704.

[4] V. Zezulka, P. Straka, P. Mucha: A magnetic filter with permanent magnets on the basis of rare earth, Journal of Magnetism and Magnetic Materials, 2004, vol. 268, pp. 219–226.

[5] A.V. Sandulyak., A.A. Sandulyak, V.A. Ershova: Magnetization curve of a granulated medium in terms of the channel-by channel magnetization model (new approach), Doklady Physics (Proceedings of Academy of Sciences), 2007, vol. 413, no. 4, pp. 469–471.

[6] A.V. Sandulyak., A.A. Sandulyak, V.A. Ershova: On the model of channel-by-channel magnetization of a granular medium (with a radial permeability profile of a quasi-continuous channel), Technical Physics, 2009, vol. 54, no. 5, pp. 743–745.

[7] A.A. Sandulyak., V.A. Ershova, D.V.Ershov, A.V. Sandulyak: On the properties of "short" granular magnets with disordered chains of grains: A field between grains, Physics of the Solid State, 2010, vol. 52, no. 10, pp. 2108–2115.

Application of asymptotic averaging method for numerical analysis of functionally gradient plate

M.I. Savenkova[1], S. V. Sheshenin[2*]

[1] Faculty of Mechanics and Mathematics, Leninskiye Gory 1, Main building, Lomonosov Moscow State Univesity, 119991 Moscow, GSP-1, Russsia

[2] Faculty of Mechanics and Mathematics, Leninskiye Gory 1, Main building, Lomonosov Moscow State Univesity, 119991 Moscow, GSP-1, Russsia

Abstract

Layered composites are widely used. For example, a layer of ceramic may be bound to the metal surface to form a heat-insulating coating at high temperatures. However, the contrast material properties result in the appearance of the high stresses and strains followed by the plastic flows in the metal phase, delamination and cracking [1]. The way to get rid of these difficulties is the use of functionally graded materials (FGM).
The two-scale method of asymptotic averaging allows both calculating the effective properties of FGM and evaluating stresses and strains. The developed method was applied by authors to tension-bending elasto-plastic problem for the plate of FGM [2]. An efficient parallel solution algorithm is also devised and implemented as home-made code. Numerical tests show its high parallel capability.

1 Section 1

We consider quasi static coupled tension-bending problems for layered plates made or plates made of FGM. Composite material is considered to be elastic or elasto-plastic. Asymptotic averaging uses 3D boundary-value problem as starting point. First of all, loading process uses loading parameter called time that allows identifying any loading instance. As usual, time discretization leads to time steps and incremental approach. Certainly, only one time step is needed in the case of linear elasticity.

Figure 1 shows typical problem under consideration. The asymptotic solution at every loading step is explained below. The 3D displacements at any time step are represented as asymptotic expansion. It is rigorously proved that 3D problem is reduced to two kinds of problems at each time step. The problems of the first type are 1D problems and are formulated in terms of ksi coordinate (called fast coordinate) in across-the thickness direction (see fig. 1) for any coordinates x,y. Therefore, solution of the local problems depends on coordinates x,y as parameters. In practice discretization along x and y coordinate is used.

*Corresponding author: S.V. Sheshenin, e-mail: sheshenin@mech.math.msu.su

The local problems can be easily solved numerically for all discrete x,y coordinates in parallel with high level of efficiency. The local problems solutions gives a way to calculate average (or effective) tangent stiffnesses that depend on x,y coordinates.

The second kind of problem is the global problem formulate for the entire plate. In general it is formulated as coupled tension-bending problem of Kirchhoff type theory. Tangent stiffnesses serve as coefficients in global equations. After the global problem is solved, displacements, stresses and strains are calculated as sums of global and local components.

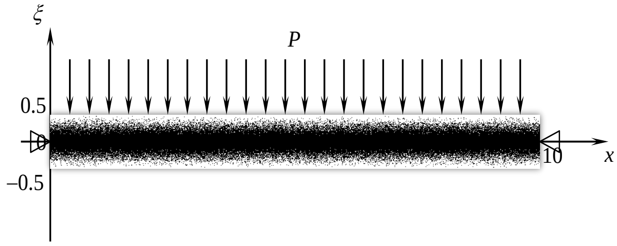

Figure 1. Bending of simple supported plate.

Numerical examples of the technique developed are given for FG material that consists of metal and ceramic components. An advantage of FGM compared to layered material in terms of stress smoothness is illustrated.

2 Conclusion

A new version of the asymptotic method of averaging for tension-bending problems for plates is proposed as well as efficient parallel implementation. The implementation exploits explicit or implicit Euler-like methods. The proposed version of the asymptotic averaging method is developed for in-plane periodic plates made of nonlinear composite materials. It is illustrated by the example of elastic-plastic bending of laminated plates and plates of functionally gradient materials.

References

[1] Finot M. and Suresh S., "Small and large deformation of thick and thin-film multi-layers: effects of layer geometry, plasticity and compositional gradients," Journal of the Mechanics and Physics of Solids, vol. 44, no. 5, pp. 683-721, 1996.

[2] Sheshenin S.V., Savenkova M.I. Averaging for non-linear problems in composite mechanics, Vestnik Moskovskogo universiteta, 1, Mathematics and Mechanics, № 5, pp. 58-62, 2012.

Mathematical modelling of stack piezoelectric generator

A. Soloviev[1,2*], V. Chebanenko[3]

[1] Don State Technical University, Gagarin sq., 1, Rostov-on-Don, 344000, Russia

[2] I. I. Vorovich Institute of Mathematics, Mechanics and Computer Sciences, Southern Federal University, Milchakov st., 8A, Rostov-on-Don, 344090, Russia

[3] Southern Scientific Center of Russian Academy of Science, Chekhov st., 41, Rostov-on-Don, 344006, Russia

Abstract

Results of mathematical modeling of the stack type piezoelectric generator (PEG) in the energy harvesting device are presented here. The considered PEG is a multilayer axisymmetric piezoceramic package. In order to model this device, semi-analytical model based on the extended Hamilton's principle was developed. Numerical results were compared with the experimental data on the low-frequency pulse excitation of stack PEG and showed a good convergence.

1 Mathematical model

Recently, attention has been directed to analytical studies of stack type generators. Due to the axial PEGs can carry sufficiently high compression stresses that allows their integration in different infrastructure objects (for example, transport automobile roads and rail-roads) then there is necessity to develop mathematical models for prediction of output characteristics of PEGs.

Several models of stack type PEG have been proposed in [1, 2]. Model presented in [1] depends on initial experimental data and does not provide information about displacements. Model proposed in [2] does not have such disadvantages. Nevertheless, it is very tedious for analysis due to its recursive type. Therefore, on the base of extended Hamilton's principle along with assumed modes method for N modes we have developed semi-analytical model (see Fig.1a):

$$\begin{cases} \mathbf{M}\ddot{\boldsymbol{\eta}}(t) + \mathbf{D}\dot{\boldsymbol{\eta}}(t) + \mathbf{K}\boldsymbol{\eta}(t) - \boldsymbol{\Theta} v(t) = \mathbf{p}, \\ Cv(t) + \boldsymbol{\Theta}^T \boldsymbol{\eta}(t) = -v(t)/R, \end{cases}$$

$$C = N\frac{S}{h}Э_{33}^{S*}, \quad K_{ij} = \int_0^H EI\phi_i'(x_3)\phi_j'(x_3)dx_3, \quad \Theta_i = \int_0^H J_p\phi_i'(x_3)dx_3,$$

$$M_{ij} = \int_0^H m\phi_i(x_3)\phi_j(x_3)dx_3, \quad p_i = -p_0\phi_i(x_3), \quad EI = \iint_S c_{33}^{E*}dS, \quad J_p = \iint_S \frac{e_{33}^*}{h}dS.$$

where $\eta_k(t)$ and $v(t)$ – unknown generalized coordinates and voltage respectively, C – effective capacitance, M_{ij} – elements of the mass matrix, K_{ij} – elements of stiffness matrix, Θ_i – elements of electromechanical coupling vector, p_i – effective mechanical load vector, $\phi_i(x_3)$ – known cinematically admissible trial functions that satisfy the

*Corresponding author: A. N. Soloviev, e-mail: solovievarc@gmail.com

boundary conditions, R – resistive load, EI – sectional rigidity, m – specific weight, h – height of the one piezoelectric layer, H – height of the stack, S – cross-section area, $э_{33}^{S*}$, c_{33}^{E*}, e_{33}^{*} – material constants of piezoelectric body.

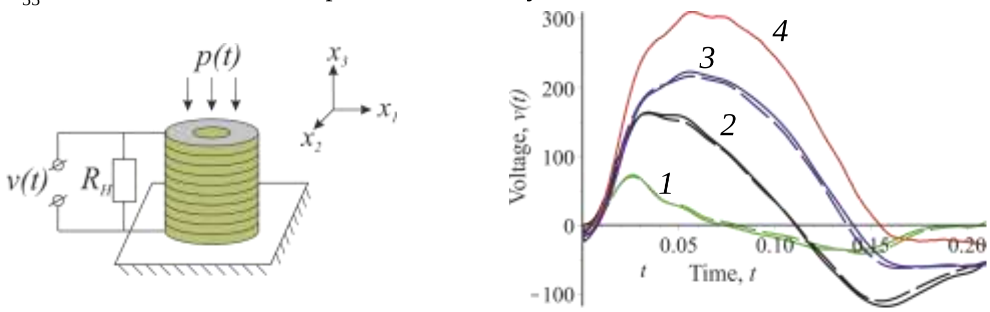

a) b)

Figure 1. Mathematical model of PEG: a) – scheme of model, b) experimental (dashed line) and numerical (solid) voltages for different resistive loads.

2 Experimental validation

In order to verify proposed model experiments on the low-frequency pulse excitation of stack PEG were held [3]. Form of mechanical loading impulse was recorded with the help of ADC L-Card E14-440. Then by using Fourier approximation this impulse was used as a mechanical loading in the proposed model (see curve 4 on Fig. 1b. 1 *V* = 1 *kgF*). Results of the calculated voltages along with the experimental ones are presented on Fig. 1b: 1 – resistive load is equal to 374 *kOm*, 2 – 2.5 *MOm*, 3 – 22.7 *MOm*. Results from Fig. 1b showed good convergence with the experimental data.

3 Conclusion

Semi-analytical model based on the extended Hamilton's principle was developed for multilayered stack PEG. Comparison between calculated results and experimental data on the low-frequency pulse excitation of stack PEG showed a good convergence.

The study was partly supported by the government contract (project part) 9.1001.2017/PCh

References

[1] S. Zhao, A. Erturk, Deterministic and band-limited stochastic energy harvesting from uniaxial excitation of a multilayer piezoelectric stack, Sensors and Actuators A: Physical, 2014, vol. 214, pp. 58–65.

[2] J. Wang, Z. Shi, Z. Han, Analytical solution of piezoelectric composite stack transducers, Journal of Intelligent Material Systems and Structures, 2013, vol. 24(13), pp. 1626–1636.

[3] V.A. Akopyan, I.A. Parinov, Yu.N. Zakharov, V.A. Chebanenko and E.V. Rozhkov. Chapter 24. Advanced Investigations of Energy Efficiency of Piezoelectric Generators. In. Advanced Materials – Studies and Applications, 2015, pp .417–436

Modelling of dielectric elastomers accounting for electrostriction by means of a multiplicative decomposition of the deformation gradient tensor

E. Staudigl and M. Krommer

Research group Mechanics of Solids
Institute of Mechanics and Mechatronics, TU Wien
Getreidemarkt 9, A-1060 Vienna, Austria

Abstract

Nonlinear modeling of the inelastic behavior of materials by a multiplicative decomposition of the deformation gradient tensor is quite common for finite strains. The concept has proven applicable in thermoelasticity, elastoplasticity, as well as for the description of residual stresses arising in growth processes of biological tissues [1]. In the context of advanced materials, electro-elastic elastomers have been investigated in [2], shape-memory alloys in [3] and piezoelastic materials in [4]. In the present paper we apply this multiplicative approach to the special case of dielectric elastomers in order to account for the electrostrictive effect. Therefore, we seek to include the two main sources of electro-mechanical coupling in dielectric elastomers as pointed out in [5] - elastostatic forces acting between the electric charges and electrostriction due to intramolecular forces of the material. In particular we intend to study the significance of electrostriction for the particular case of dielectric elastomers in the form of a thin layer with two compliant electrodes.

1 Extended summary

Our approach uses the well known governing equations of three-dimensional non-linear electroelasticity (see [6]) as a starting point. We briefly review these relations following their presentation as given in [7], and introduce the concept of the multiplicative decomposition of the deformation gradient tensor into two parts; the electrical part $\mathbf{F}_{el}$ and the mechanical part $\mathbf{F}_{me}$, such that $\mathbf{F} = \mathbf{F}_{me} \cdot \mathbf{F}_{el}$. Here, the electrical part depends on the material electric field $\boldsymbol{\mathcal{E}}$, it accounts for electrostriction and it results into an intermediate configuration, in which the mechanical part of the stress tensor vanishes. This configuration is usually interpreted as a configuration of the material body, which results from de-stressing the deformed material body. Such a de-stressing is obtained by releasing the body from its support, and by removing all body forces and body couples as well as the tractions; here, also the electrical contributions to body forces, body couples and tractions are included. Moreover, the body is fictitously cut into infinitesimally small bodies from which the stresses at the surface are removed as well. In general, this intermediate configuration resulting from electrostriction by means of $\mathbf{F}_{el}$ does not physically exist for the material body; on the one hand side, because it might be incompatible, and on the other hand side, because the electric field also results into a polarisation of the material producing body forces, body couples and tractions. Yet, the intermediate configuration plays an imperative role in the constitutive modelling. In particular it enables the additive decomposition of the free energy into a purely mechanical part Ψ_{me} and an electrical part Ψ_{el}. In combination with an augmentation term Ψ_{aug}, the augmented free energy Ω is

$$\Omega = \Psi_{me}(\mathbf{C}_{me}) + \Psi_{el}(\mathbf{C}, \boldsymbol{\mathcal{E}}) + \Psi_{aug}(\mathbf{C}, \boldsymbol{\mathcal{E}}). \quad (1)$$

$\mathbf{C}$ ist the right Cauchy-Green tensor and $\mathbf{C}_{me} = \mathbf{F}_{me}^T \cdot \mathbf{F}_{me}$ its mechanical part. The so-called second Piola-Kirchhoff total stress $\mathbf{S}_t$, which is the sum of the mechanical stress $\mathbf{S}$, the polarization stress $\mathbf{S}_p$ and the Maxwell stress $\mathbf{S}_m$, and the material electric displacement vector $\boldsymbol{\mathcal{D}} = \boldsymbol{\mathcal{P}} + \varepsilon_0 J \mathbf{C}^{-1} \cdot \boldsymbol{\mathcal{E}}$ involving the material polarization $\boldsymbol{\mathcal{P}}$ can be computed from

$$\mathbf{S}^t = 2\frac{\partial \Omega}{\partial \mathbf{C}} - p\mathbf{C}^{-1} \quad \text{and} \quad \boldsymbol{\mathcal{D}} = -\frac{\partial \Omega}{\partial \boldsymbol{\mathcal{E}}}. \quad (2)$$

As dielectric elastomers are nearly incompressible, we model them as incompressible; this constraint is implemented by means of the Lagrange multiplier p in the constitutive relation for the total stress tensor. As a specific form of the augmented free energy we use

$$\Omega = \Psi_{me}(\mathbf{C}_{me}) - \frac{1}{2}\chi\varepsilon_0 \boldsymbol{\mathcal{E}} \cdot \left(\mathbf{C}^{-1} \cdot \boldsymbol{\mathcal{E}}\right) - \frac{1}{2}\varepsilon_0 J \boldsymbol{\mathcal{E}} \cdot \left(\mathbf{C}^{-1} \cdot \boldsymbol{\mathcal{E}}\right). \tag{3}$$

In this formulation for the augmented free energy we have accounted for the isotropy of the dielectric elastomer. The last term is $\Psi_{aug}(\mathbf{C}, \boldsymbol{\mathcal{E}})$ and the center term is $\Psi_{el}(\mathbf{C}, \boldsymbol{\mathcal{E}})$; for $\Psi_{me}(\mathbf{C}_{me})$ any hyperelastic strain energy function which is typically used for purely mechanical isotropic and incompressible materials may be used and $\mathbf{C}$ is simply replaced by $\mathbf{C}_{me}$. Eventually, we introduce the electrical part of the deformation gradient tensor as a symmetric stretch tensor

$$\mathbf{F}_{el} = \mathbf{U}_{el} = \lambda_{el}\mathbf{ee} + \lambda_{el}^{-1/2}\left(\mathbf{I} - \mathbf{ee}\right), \tag{4}$$

in which the electric field is $\boldsymbol{\mathcal{E}} = \mathcal{E}\mathbf{e}$ and the electrical stretch is $\lambda_{el} = \lambda_{el}(\mathcal{E}^2) = \lambda_{el}(\boldsymbol{\mathcal{E}} \cdot \boldsymbol{\mathcal{E}})$; also the incompressibility of the material has been accounted for. The specific form of λ_{el} is yet to be determined. For that sake the simple problem of a capacitor filled with a dielectric elastomer is studied under the assumption of a homogenous electric field $\boldsymbol{\mathcal{E}} = \mathcal{E}\mathbf{e}$ in the direction $\mathbf{e}$ perpendicular to the plane of the capacitor and with $\mathcal{E} = const$. Moreover, a homogenous incompressible deformation $\mathbf{F} = \lambda\mathbf{ee} + \lambda^{-1/2}\left(\mathbf{I} - \mathbf{ee}\right)$ is assumed. Under these assumptions the total stress tensor vanishes and solving this simple problem results into a nonlinear relation between the thickness stretch λ and the square of the applied electric field $\mathcal{E}^2$, from which we identify the constitutive equation for $\lambda_{el}(\boldsymbol{\mathcal{E}} \cdot \boldsymbol{\mathcal{E}})$ by a comparison with experimental results. Once λ_{el} has been identified one can proceed to the derivation of a nonlinear theory for dielectric elastomer plates and shells. This is left for future research.

Acknowledgement Support from the K2 area of the Linz Center of Mechatronics GmbH is gratefully acknowledged. This area is promoted as a K2 project with the project name Austrian Competence Center of Mechatronics - ACCM in the context of Competence Centers for Excellent Technologies (COMET) by BMVIT, BMWFJ and by the country Upper Austria.

References

[1] V.A. Lubarda. Constitutive theories based on the multiplicative decomposition of deformation gradient: Thermoelasticity, elasto-plasticity, and biomechanics, *Applied Mechanics Review*, 57(4): 95–108, 2004.

[2] S. Skatulla, C. Sansour, and A. Arockiarajan. A multiplicative approach for nonlinear electro-elasticity, *Computer Methods in Applied Mechanics and Engineering*, 245-246: 243–255, 2012.

[3] J. Arghavani, F. Auricchio, R. Naghdabadi, A. Reali, and S. Sohrabpour. A 3D finite strain phenomenological constitutive model for shape memory alloys considering martensite reorientation, *Continuum Mechanics and Thermodynamics*, 22(5): 345–362, 2010.

[4] A. Humer, and M. Krommer. Modeling of Piezoelectric Materials by Means of a Multiplicative Decomposition of the Deformation Gradient, *Mechanics of Advanced Materials and Structures*, 22(1-2): 125–135, 2015.

[5] M. Mehnert, M. Hossain, and P. Steinmann. On nonlinear thermo-electro-elasticity, *Proceedings of the Royal Society A*, 472: 20160170. 2016.

[6] R.A. Toupin. The Elastic Dielectric, *Journal of Rational Mechanics and Analysis*, 5(6): 849–915, 1956.

[7] A. Dorfmann, and R.W. Ogden. Nonlinear electroelasticity, *Acta Mechanica*, 174: 167–183. 2005.

Transport of saturation in liquid composite molding based on a two-phase porous flow model

F. Trochu[1*], Ll. Gascon[2], J.A. Garcia[2]

[1] Chair on Composites of High Performance (CCHP), Mechanical Engineering Department, Center of Research on Polymers and Composites (CREPEC), École Polytechnique de Montréal, Montréal, Canada, H3C 3A7,

[2] Instituto del Diseño para la Fabricación (IDF), Universidad Politécnica de Valencia. Camino Vera s/n, 46022, Valencia, Spain

Abstract

The numerical simulation of void formation during mold filling in Liquid Composite Molding (LCM) requires solving the hyperbolic transport equation describing the progressive saturation of the fibrous reinforcement in time. The liquid flow is usually modeled by Darcy's law, where permeability is a characteristic parameter of the fiber bed considered as a porous medium. In this work, a two-phase flow model resin/air, where air is assumed to be slightly compressible and resin incompressible, is coupled with Darcy's law and mass conservation to simulate the unsaturated flow. These equations lead to a system composed of a nonlinear advection-diffusion equation for saturation including capillary effects and an elliptic equation for pressure and velocity. The relative permeability of the fiber bed is introduced as a function of saturation and air density. The hyperbolic nature of the saturation equation and its strong coupling with Darcy equation through relative permeability represent a challenging numerical issue. A detailed analysis of different relative permeability models is performed. The elliptic pressure equation is solved by finite elements and the saturation equation by a modified flux limiter technique. To validate the model, the numerical solution is compared with the experimental saturation measured in a transparent mold containing a fiber glass reinforcement injected at constant flow rate. Although the numerical model provided an excellent prediction of the experimental saturation profiles in time, an experimental factor representing the amount of air entrapped in the fiber bed still needs to be investigated.

[*] Corresponding author: F. Trochu, e-mail: trochu@polymtl.ca

Mixed Eulerian-Lagrangian description in the finite element modelling of an endless metal belt system

Yu. Vetyukov[1*], M. Krommer[1]

[1] Vienna University of Technology, Getreidemarkt 9, 1060 Vienna, Austria

Abstract

We present a novel mathematical model of an endless steel belt, moving between two rotating drums. Non-cylindrical geometry of the belt, frictional contact with the moving drum surfaces, long free spans in comparison to the size of the drums make this practically relevant problem particularly challenging especially for low tension forces, when the exact geometric treatment is important for predicting various nonlinearities and buckling behavior. The proposed mixed Eulerian-Lagrangian kinematic description in the finite element model of a material surface of the steel belt along with the specific problem-oriented coordinate system allow overcoming the difficulties, which are inherent for conventional modelling strategies.

1 Statement of the problem

As depicted in Fig. 1, left, we consider a thin steel belt in contact with two rotating drums. Imperfect geometry of the belt and of the drums, gravity, slipping in the contact zones result in the complicated behavior of the structure. In the practice, the distance between the drums may exceed their radii by the factor 70 and more, and various undesired phenomena are observed in the course of the motion of the system. Thus, S-formed configurations of the belt in the plane *xy* are developing in the free spans, the belt slips to the side (*x* direction in the figure), the contact patch on the surface of the drums becomes unsymmetric with large slipping zones, etc. Designing automatic control systems requires reliable and efficient mechanical simulations, which presently are available only for tightly spanned belts. We aim at a simulation scheme, which retains reliability for slack belts with prominent geometrically nonlinear effects in the long spans because of the unsymmetric contact interaction, and which would not suffer from the numerical polygon effect because of finite elements travelling from free spans to contact zones and back.

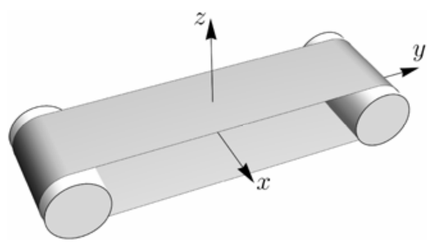

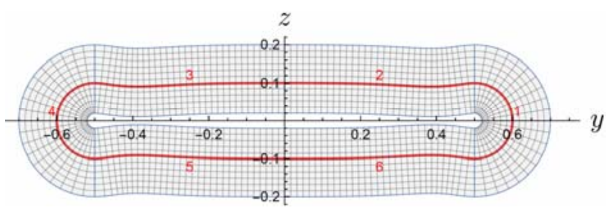

Figure 1. Left: schematic model of a steel belt, spanned on two drums; right: problem-specific coordinate system

*Corresponding author: Yury Vetyukov, e-mail: yury.vetyukov@tuwien.ac.at

2 Mathematical model

While axially moving structures are traditionally modelled with certain geometric simplifications [1-3], recently the mixed Eulerian-Lagrangian description was proven efficient for geometrically exact treatment of moving continua [4-5]. Combining these ideas with the scheme of a contour motion of a belt drive [6], we represent the kinematics using a compound coordinate system (Fig. 1, right) with necessary degree of continuity. The transverse coordinate in *yz* plane as well as the material coordinate of a belt particle become functions of the circumferential (Eulerian) coordinate and time. A planar finite element model of a belt drive with large displacements, stick and slip in the contact zones and material particles, travelling across the finite element mesh has been developed and successfully tested. In Fig. 2, left, the nodes of the mesh are marked blue, and the green and yellow colors answer to the slipping and sticking contact. Currently, an extension towards a three-dimensional model of a steel belt as a material surface with membrane and bending stiffness is under development, see Fig. 2, right. Preliminary results are available, and the numerical efficiency as well as the model of friction require further research work.

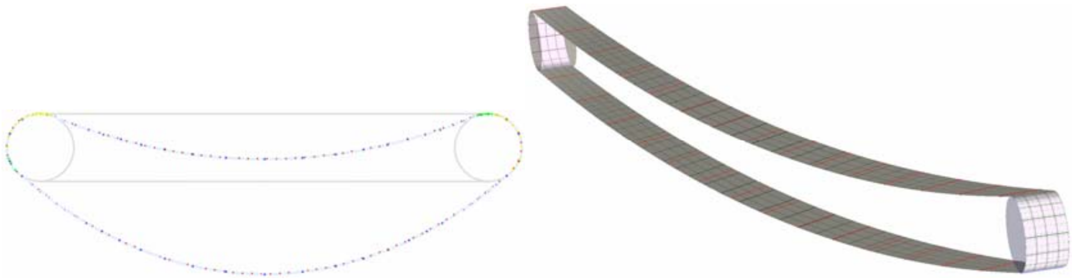

Figure 2. Left: planar mathematical model with the belt as a string;
right: finite element model of the material surface of the belt

References

[1] L.-Q. Chen. Analysis and Control of Transverse Vibrations of Axially Moving Strings, ASME Applied Mechanics Reviews, 2005, vol. 58, pp. 91–116.

[2] J. Wickert, C. Mote. Classical vibration analysis of axially moving continua, Journal of Applied Mechanics, 1990, vol. 57, pp. 738–744.

[3] M. H. Ghayesh, M. Amabili, M.P. Païdoussis. Nonlinear dynamics of axially moving plates, Journal of Sound and Vibration, 2013, vol. 332, pp. 391–406.

[4] Yu. Vetyukov, P. Gruber, M. Krommer. Nonlinear model of an axially moving plate in a mixed Eulerian-Largangian framework, Acta Mechanica, 2016, vol. 227, pp. 2831–2842.

[5] Yu. Vetyukov, P. Gruber, M. Krommer, J. Gerstmayr, I. Gafur, G. Winter. Mixed Eulerian-Lagrangian description in materials processing: deformation of a metal sheet in a rolling mill, International Journal for Numerical Methods in Engineering, early view, 2016, pp. 1–20.

[6] V. Eliseev, Yu. Vetyukov. Effects of deformation in the dynamics of belt drive, Acta Mechanica, 2012, vol. 223, pp. 1657–1667.

Free Vibration Analysis of Beams with Piezo-Patches Using a One-Dimensional Model with Node-Dependent Kinematic

E. Zappino[1*], E. Carrera[1], G. Li[1]

[1] Politecnico di Torino, Corso Duca degli Abruzzi, 24, 10129 Turin, Italy

Abstract

The electro-mechanical analysis of beams with piezo-patches requires accurate models to be used. The interface between the beam and the patch has to be modeled properly to provide accurate results. The use of refined one-dimensional models may lead to a high accuracy in the solution when an appropriate kinematic model is used, as shown by Miglioretti and Carrera [1]. Nevertheless, refined kinematic models require a high number of degrees of freedoms that increase the computational cost of the analyses. The use of advanced models only in the portion of the structure where high accuracy is required, e.g. the patch area, could reduce the computational cost preserving the results accuracy. Biscani *et al.* [2] proposed the use of the Arlequin method to study the two-dimensional structures with piezo-patches coupling models with different kinematics.

This paper presents a new class of advanced one-dimensional models with node-dependent kinematics for the dynamic analysis of beam structures with piezo-patches. ESL (Equivalent Single-layer) models and LW (Layer-wise) models have been taken into account. The Carrera Unified Formulation [3], has been used to derive the model in a compact and general form. The Finite Elements Method has been used to solve the one-dimensional problem. The cross-sectional kinematic approximation has been considered as a function of the one-dimensional element node [4], that is, no *ad-hoc* techniques have been used to derive the node-dependent kinematic model. Governing equations for beam models with node-dependent kinematics accounting for electromechanical effects are derived from the Principle of Virtual Displacement (PVD).

The free vibration analysis of various beams structures with piezo-patches has been performed. The results obtained have been compared with solutions taken from literature. When used in the analysis of structures with local components or effects to be accounted for, the proposed advanced models can bridge the locally refined model to the global model and reduce the computational costs significantly while guarantying accuracy without employing special global-local coupling method.

[*]Corresponding author, e-mail: enrico.zappino@polito.it.

References

[1] Miglioretti, F., Carrera, E. 2015. Application of a Refined Multi-Field Beam Model for the Analysis of Complex Configurations. Mechanics Of Advanced Materials And Structures, 22(1-2), pp.52-66.

[2] Biscani, F., Nali, p., Belouettar, S. and Carrera E. 2012,Coupling of hierarchical piezoelectric plate finite elements via Arlequin method.Journal of Intelligent Material Systems and Structures, 23(7), pp. 749-764.

[3] Carrera, E., Cinefra, M., Petrolo, M. and Zappino, E. 2014. Finite Element Analysis of Structures through Unified Formulation. John Wiley & Sons.

[4] Carrera, E., Zappino, E. 2014. Analysis of complex structures coupling variable kinematics one-dimensional models. ASME International Mechanical Engineering Congress and Exposition, IMECE 2014. Montreal, Canada, 14 - 20 November 2014